Mechanical and adaptive behaviour of bone in relation to hip replacement.

A study of bone remodelling and bone grafting

Sébastien Muller

Department of structural engineering
Faculty of engineering science and technology
Norwegian university of science and technology

Norwegian orthopaedic
implant research unit
St Olavs Hospital

Trondheim, january, 2005

Department of structural engineering
Faculty of engineering science and technology
Norwegian university of science and technology
Trondheim, Norway

ISBN 82-471-6933-9 (printed version)
ISBN 82-471-6932-0 (electronic version)
ISSN 1503-8181

Printed by NTNU-trykk

NTNU-trykk, Dragvoll
N-7491 Trondheim
Tel.: +47-73 59 66 53 or 54
Fax: +47-73 59 76 29

Summary

This thesis, consisting of an introduction and four separate papers, gathers considerations on bone behaviour in relation to total hip replacement. Aspects related to primary hip replacement, principally adaptive bone remodelling, are addressed in Paper I from a clinical point of view and in Paper II from a mechanical point of view. Morsellised bone applied in secondary hip replacement is studied in Paper III, where its recoil is modelled as viscoelastic, while Paper IV questions the validity of a solid model for this material.

The relationship between preoperative bone stock and relative postoperative change of bone amount was investigated in Paper I. Younger patients with custom uncemented femoral implants who had high preoperative bone stock had more bone loss than those with low preoperative bone stock. This unexpected result around the hip is nevertheless an accepted result in knee replacement. Also a new graphic interpretation of the paired variations of bone mineral density and projected bone area showed that bone tends to remodel after surgery to reach a lower density and a higher volume.

The main purpose of Paper II was to connect mechanical stimulus to the remodelling observed in the same patients as in Paper I. Bone remodelling was simulated individually and compared with the clinical measurements in the corresponding patient. An additional modelling of a hypothesised fading memory of the bone was implemented to an established set of equations connecting mechanical stimulus to remodelling. Comparisons at a global level of simulated and clinical results showed that simulations have a good predictive value but are not quantitatively correct prior to statistical processing. The observed discrepancy suggested an improvement of the material modelling.

The recoil behaviour of morsellised bone is of great clinical relevance for the primary stability of revision implants. The aim of Paper III was threefold: derive from experiments clinically relevant material parameters, use these to discriminate the effect of pre-treatment of the bone grafts on their recoil properties, and compare these outcomes to loading properties. The experimental unloading was a model using a linear viscoelastic solid model from which three parameters were derived describing the swelling retardation, the swelling speed and the amount of swelling. They allowed the identification of significant effects of water content and particle size on the recoil of morsellised bone. Two of the parameters correlated to loading properties.

The protocol used in Paper III investigates only part of the behaviour of morsellised bone. A different geometry and load modus was studied in Paper

IV. Impacted morsellised bone in a cavity mimicking the femoral canal was loaded axially and with torsion. The experiment was modelled with finite elements using the same material modelling as in Paper III, a linear viscoelastic solid model. Though the simulation captured the gross features of the response of bone grafts to loading, it did not achieve displacements as large as in the experiments. This suggested that the pulverulent behaviour of morsellised bone dominated in this load case, allowing it to flow under load, which indicates that fluid viscoelasticity could be a better model for bone grafts.

Acknowledgements

This work has been carried out at the Norwegian orthopaedic implant research unit (NOIRU) in Trondheim, Norway as a doktor ingeniør degree at the Norwegian university of science and technology, departement of structural engineering.

I would like to thank Eivind Andersen and Are Funderud who introduced me to the biomechanics of the hip. Their work on customised uncemented implants started my interest for the mechanics of bone tissue.

My supervisor Professor Fridtjov Irgens has followed me from my very beginnings in biomechanics, listenning patiently to my stammering norwegian at first and always soothing my anguish at later stages of my work. His enormous contribution to the teaching of mechanics in Norway and abroad has been a model to find the motivation for more work.

I also would like to express my ackowledgement to Professor MD Pål Benum and PhD MD Arild Aamodt for their faith in my work, their financial support through NOIRU and their advisory support throughout my work.

Thank you to Kristin Haugan and Jomar Klaksvik at NOIRU for their permanent help on technical or administrative issues during my PhD or more general "life issues".

During my five-month stay at the Orthopaedic research lab in Nijmegen, the Netherlands, I learnt a lot about bone remodelling simulation. For this as well as for their warm welcome, I would like to thank PhD Nico Verdonschot, Marco Barink, PhD Jan Stolk, PhD Marieke Willems, René van der Venne, and Ineke Huidekoper.

Special thanks to my dear sister Rita for her permanent closeness despite the many kilometers between us. Thank you for your unconditionnal support every single day I have been working on this PhD.

Finally, I wish to express my gratitude to Arne for enduring my humour changes due to successive postponing of the accomplishement of this work. Thank you for your encouragements, your faith in me, and your bringing me back to reason so often.

Trondheim, january 2005

Sébastien Muller

Contents

Summary **i**

Acknowledgement **iii**

1 Bone **1**
1.1 Living bone . . . 1
1.1.1 Bony tissues and cells . . . 1
1.1.2 Mechanical modelling of living bone . . . 3
1.2 Morsellised bone . . . 4
1.2.1 Description and biological considerations . . . 4
1.2.2 Mechanical considerations . . . 4

2 Hip operations **5**
2.1 Total hip replacement . . . 5
2.1.1 Uncemented femoral implants . . . 6
2.1.2 Periprosthetic bone remodelling . . . 7
2.2 Revision . . . 8

3 Bone remodelling **9**
3.1 The physiological processes . . . 9
3.1.1 Load bearing and change in bone mass . . . 9
3.1.2 Cellular mechanisms . . . 10
3.2 Modelling mechanically induced bone remodelling . . . 10

4 Computational and imagery techniques **12**
4.1 The finite element method in biomechanics . . . 12
4.1.1 The finite element method (FEM) . . . 12
4.1.2 Applications to tissue mechanics . . . 13
4.2 Dual energy x-ray absorptiometry (DEXA) . . . 14
4.2.1 Basic principles . . . 14
4.2.2 Gruen zones . . . 14
4.3 Computer tomography . . . 16

Summary of papers **19**

References **21**

Paper I A quantitative and qualitative analysis of bone remodelling around custom uncemented femoral stems: a five-year DEXA follow-up

Paper II Comparison of patient-specific bone remodelling simulation and five-year *in vivo* DEXA measurements

Paper III Viscoelastic modelling of impacted morsellised bone accurately describes unloading behaviour: an experimental study of stiffness moduli and recoil properties

Paper IV Morsellised bone under compression and torsion in femoral canal-like cavity: comparison of finite element simulations and experimental data

Introduction

1 Bone

This thesis considers various aspects of the behaviour of bone in connection with hip replacement, as a living and adaptive tissue and as a dead material. Thus, understanding some elements of bone structure and physiology might help our understanding of both the modelling of the bone's mechanical properties and the processes underlying its ability to accommodate to its environment. Only the main structures in adult normal bone are considered here.

1.1 Living bone

1.1.1 Bony tissues and cells

At a macroscopic level there are two different structures of bone: cortical or compact bone and trabecular or cancellous bone. Cortical bone is found essentially in the shaft of long bones and represents 80 % of the skeleton. Cortical bone is a compact material; non-cellular matter occupies 95 % of the total volume and blood vessels and cells occupy the remaining 5 %. Cancellous bone is found mainly in the end of long bones, in vertebras and flat bones. It represents 20 % of the skeleton and consists of a porous network of trabeculae interconnected in a honeycomb pattern where bone matter occupies only 20 % of the total volume (Figure 1). The free space is filled with bone marrow and blood vessels. This spongious structure gives trabecular bone a large surface to volume ratio of $20\,mm^2/mm^3$ vs. only $2.5\,mm^2/mm^3$ in compact bone (Eriksen et al., 1993). As most metabolic activity takes place at free bone surface, the skeletal turnover is three to ten times more rapid in cancellous than in cortical bone (Sambrook, 2001).

At a lower level of structure, compact bone consists mainly of cylindrical canals of concentrically arranged lamellae around blood vessels. These canals, called Harvesian systems or osteons, are aligned longitudinally (for long bones) and the cavity inside has a diameter of $100\,\mu m$ (Currey, 1984). In between osteons, interstitial lamellae are found with layers randomly oriented from one location to another.

The lamellar bone matrix is a highly organised material (de Ricqles et al., 1991). Collagen fibrils are packed closely and parallel with crystals of hydroxyapatite regularly distributed along the length of the fibres. The plywood-like

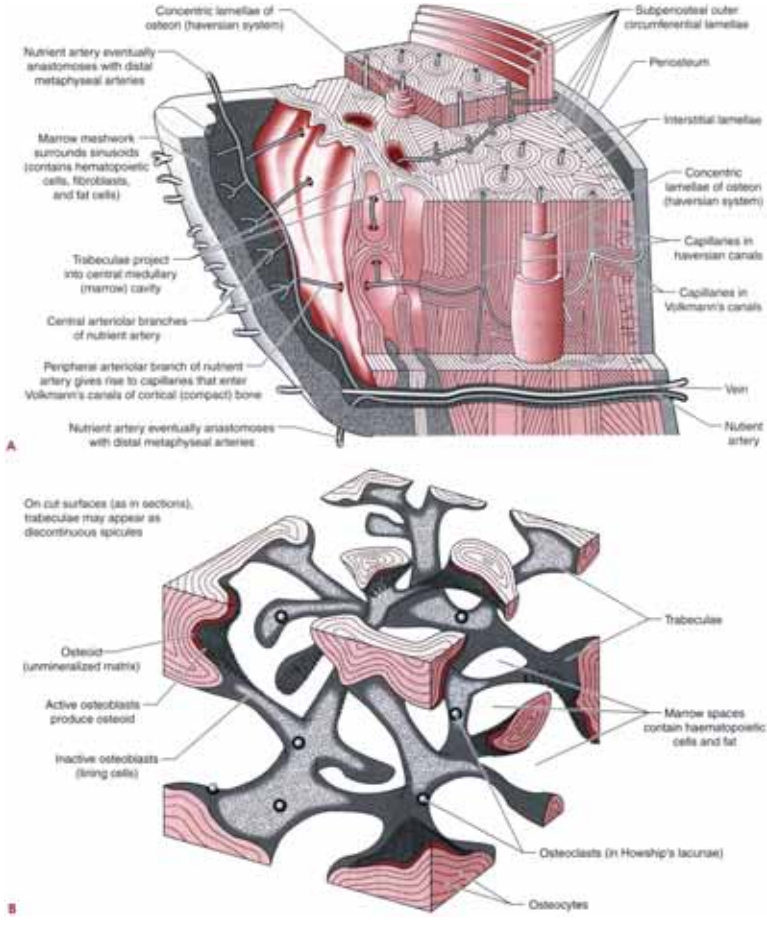

Figure 1: Cortical bone structure with focus on the Harvesian systems (A). Cancellous bone structure with osteoblasts, osteoclasts and osteocytes (B). Reproduced from (Sambrook, 2001)

structure of lamellar bone can be either an orthogonal plywood structure with fibre directions changing by 90° between two consecutive lamellae or a twisted plywood-like structure with a regular rotation of a given angle between consecutive lamellae (Giraud-Guille, 1988).

Within those structures lie different types of cells: osteoclasts are responsible for bone resorption and osteoblasts are responsible for bone formation. Osteoblasts are located on free bone surfaces distributed among covering cells. Some osteoblasts are incorporated into the bone matrix and become osteocytes and are able to communicate both with each other and with osteoblasts.

1.1.2 Mechanical modelling of living bone

Constitutive models of mechanics rely on the basic hypothesis that the material to be described is a continuum. Modelling a discontinuous material as a continuum limits the validity of the predicted results to the length scale on which the material properties are averaged (Cowin, 1993). Rauber in the 19^{th} century was aware of the fact that "strength of bone is dependent upon the material, the microscopic structure and the shape of the whole bone" (Rauber, 1876). In spite of this awareness, the largest part of the biomechanical data were gathered between 1955 and 1973 using common testing methods in engineering design that focused on external influences and that regarded microstructure as less important (Roesler, 1987). This contributed to an understanding of bone as a material rather than a structure. Consideration of anisotropy, already suggested in 1957, was a first step toward a structural description. A transverse isotropic model for human bone was established 18 years later (Reilly and Burstein, 1975) and inhomogeneity within cortical bone was suggested a few years later by Van Buskirk and Ashman (1981). One way to overcome the limitations due to the averaging of discontinuities, was to use a homogenisation method. This method proposes to represent the discontinuous material by a continuous and homogeneous one with the same macroscopic behaviour. It can then be used to estimate back strains at the microscopic level based on macroscopic computations (Prendergast, 1997). The basic assumption is a periodic structure repeating a base cell. The mechanical properties of the basic material for the base cell and its shape and size determine the macroscopic mechanical behaviour. Though the architectural idealisation is debatable and the mechanical properties of the base cell have to be estimated, this method allows relating architectural patterns and density in trabecular bones to continuous material properties. Another type of homogenisation has been presented by Van Rietbergen et al. (1996), who

micro-scanned a cube of trabecular bone and ran a finite element analysis to estimate the corresponding macroscopic stiffness matrix.

1.2 Morsellised bone

1.2.1 Description and biological considerations

Morsellised bone consists of solid particles of cortical or cancellous bone and bone marrow, which itself may be considered as a combination of water and fat. Not only the relative amount of these components determines its behaviour but also the grading of the bone particles (Ullmark and Nilsson, 1999).

Revascularisation of the bone grafts is determinant for its integration in new bone (Kirkeby and Berg-Larsen, 1991) and hence for the success of the reconstruction. Fresh morsellised bone originated from cancellous bone is better revascularised than from cortical bone (Solheim et al., 2001). Pre-treatment as demineralisation or freezing as well as the syngeneic or allogeneic origin of the bone also influences vascularisation and mineralization. Although syngeneic bone is superior to allogeneic in respect to vascularisation and mineralization, the difference is reduced by pre-treatment (Kirkeby et al., 1992).

Bone grafts can also be impregnated locally with antibiotics to diffuse them massively where they are needed during the first days and weeks after operation, (Witsø et al., 1999).

1.2.2 Mechanical considerations

The nature of morsellised bone is ambiguous. As a pulverulent, it behaves both like a fluid taking the shape of its container and like a solid as it does not flow out when left on a free surface. If not pre-treated by impaction, its tension strength is virtually zero as nothing but surface tension of the fluid phase ensures the cohesion of its components. In Paper III, morsellised bone in a container was adequately modelled by a generalised Kelvin model suitable for solid, while in Paper IV, the large displacements observed experimentally and not predicted by the same material model suggested a flow of material and hence that a fluid model would be more suitable. The fact that the bone is ground suggests naturally both isotropy and homogeneity though these characteristics are only achieved at a rather macroscopic scale.

Many studies have explored the*in vivo* mechanical behaviour of bone grafts with respect to implant stability (Capello, 1994; Kärrholm et al., 1999; Pekkarinen et al., 2000). However, its mechanical properties as a material have mostly

been investigated the last five to ten years with the help of geotechnical methods usually employed to study soils. The grading of the bone particles was found to be poor by geotechnical standards as an optimal distribution should be very broad and include both finer and larger particle (Brewster et al., 1999). Study of the recoil properties by Ullmark et al. (1999) showed that finer particles and higher impaction force cause larger recoil. The new procedure followed in Paper III provides quite different results thus suggesting that the grading of the particles may matter more than their average size. This viscoelastic aspect was investigated more deeply by Giesen et al. (1999) who established the existence of large irreversible deformations caused by flow-independent creep behaviour due to rolling and sliding of the bone particles. The close relationship between confined compression modulus and permeability they showed suggests an influence the fluid content in morsellised bone. A study by Voor et al. (2004) established that uniaxial compressive strain was significantly decreased in defatted bone grafts.

2 Hip operations

2.1 Total hip replacement

In 2003, 7900 patients underwent a hip operation in Norway; these comprised 6900 first time operations (primary hip replacement) and 1000 re-operations (revision surgery) (Furnes et al., 2004). About 40 % of the patients were between 71 and 80 years old and 69 % of all patients were women. The main cause of operation was arthrosis (70 %), a degenerative joint disease with cartilage damage and loss. A secondary cause was femoral neck fracture (12 %) and hip dysplasia (8 %), an abnormal anatomic structure of the femoral head due to a growth disorder.

The stress on the joint surface is easily doubled due to changes of the shape of the femoral head and hence of the contact surface. Overweight aggravates the overload and should be kept under control. Operative treatment is indicated when the patient is in strong pain that impairs work capacity or rest (Edvardsen, 1989). The usual intervention is the total hip replacement. The acetabulum, the cup-formed part of the pelvis receiving the femoral head, is rasped and embedded with an artificial polyethylene cup. A metallic ball anchored to the femoral shaft by means of a femoral implant replaces the femoral head (Figure 2). The femoral implant is anchored itself in the marrow cavity (Steen Jensen, 1986).

Figure 2: A femoral component inserted in the femoral canal. The acetabular cup is fixed in the pelvic bone and receives the artificial femoral head.

2.1.1 Uncemented femoral implants

To anchor the hip implant in the femoral canal, two main fixation techniques are available: cemented and uncemented stems. Though uncemented implants have increased their survival percentage from 87 to 95 % in the last twelve years, they do not surpass cemented implants at a survival percentage of 97 %, when all patients are considered together (Furnes et al., 2004). Long-term results of cemented femoral stems are satisfying in younger patients though weaker results of cemented acetabular cups are reported (Callaghan et al., 1997; Kobayashi et al., 1997). However, in a randomised study comparing second generation cemented and uncemented femoral stems Bourne et al. (1995) showed no significant difference in revision rate for patients under 70 years old. They further recommended use of uncemented tapered femoral stems for patients with funnel shaped femora or with arthritis (Bourne and Rorabeck, 1998). In Norway, about 17 % of the primary operations in 2003 used uncemented femoral stems (Furnes et al., 2004).

Uncemented femoral implants usually have a porous surface covered or not by a bioactive ceramic to facilitate bone ingrowth and biological fixation. To allow proper ingrowth the micro-movements at the bone-implant interface should

not overcome $20\,\mu m$ (Jasty et al., 1997). As nothing stabilises the implant in the first weeks after operation uncemented stems rely on either press-fit stability or a so-called "fit and fill" stability (Naidu et al., 1996). The first is usually based on medullary locking where the stem is forced and locked in the distal medullary canal. Implants with good "fit and fill" try to achieve good contact with the cortical bone and to fill the femoral canal.

2.1.2 Periprosthetic bone remodelling

Medullary locking implants and implants with proximal fit provide very different load distributions on the remaining surrounding bone. Bone tissue responds to its mechanical environment by growing when loaded and disappearing when disused (see the section on bone remodelling). For medullary locking stems, as a result of the wedging effect, bone densification occurs, especially distally, which leads to reduced stresses in the proximal bone, increasing in turn the distal bearing until the proximal bone is bypassed and resorbs (Van Rietbergen et al., 1993). This phenomenon, known as stress shielding, confirmed by computer simulation of the remodelling has also been confirmed by radiographic assessment (Bugbee et al., 1997) and by DEXA measurements (Engh et al., 1992). Anatomical and custom uncemented implants are based on the "fit and fill" principle, thus focusing on an evenly distributed cortical contact and load transfer as suggested by Huiskes (1990) and Huiskes et al. (1992). Bone loss assessed by DEXA was less in the proximal regions of the femur with anatomic uncemented stems than with cemented ones (Brekelmans et al., 1972; Huiskes and Chao, 1983).

Implants with high modulus of elasticity reduce strains in the surrounding bone thus bypassing its use and enhancing stress shielding. These pure stress calculations have been confirmed by remodelling simulations (Huiskes et al., 1992). While implants with the same modulus as bone, so-called isoelastic implants, reduce stress shielding they increase proximal interface stresses thus leading to interface debonding and micromotions (Huiskes et al., 1992). Huiskes (1993) established a relation between the amount of bone loss and the ratio between the stem stiffness and the preoperative bone density, confirmed both by simulations and the clinical measurements by Engh et al. (1992).

2.2 Revision

The most important cause of revision of the femoral component is aseptic loosening. This loosening is caused by three main mechanisms: loosening at the

interface between implant and bone or implant and cement, cement breakage or breakdown of cortical structure due to bone loss or necrosis. While the lesser forms of instability can be treated by conservative procedures if no infection is suspected, instabilities involving breakage always require surgical solutions (Schneider, 1989).

In Norway in 2003, 962 patients underwent revision surgery of the hip joint, representing 12.2 % of all hip operations. The main causes were aseptic loosening of the femoral component or acetabular component (together 73 %), luxation, deep infection and pain (Furnes et al., 2004). Removal of a loose implant leaves the inner surface of the femoral canal rather smooth, which makes interlock between a new implant or cement difficult. The interface shear strength has been shown to be reduced to 21 % of the primary one (Dohmae et al., 1988). Bone loss may be so extensive that the containment of the implant and its cement mantle may be impaired (Brewster et al., 1999). Moreover the lack of proximal femoral support has been shown to significantly increase stress levels within the revision implant above its fatigue strength (Crowninshield et al., 2004). The use of bulk grafts (large pieces of bone) often caused infections and did not promote attachment of important muscles; furthermore, the grafts were not revascularised (Hooten et al., 1996). Particulate bone grafts, also called morsellised bone grafts, provide the adequate initial stability of the revision implant and are more easily vascularised and incorporated into the host skeleton (Malkani et al., 1996). Their use was first described in 1984 for restoration of bone loss in the acetabulum (Slooff et al., 1984) and in 1993 using smaller bone particles for the femur (Gie et al., 1993). To be successful, the procedure requires initial stability of the implant before new bone incorporates the grafts. Subsiding of the implant as the morsellised bone compresses is the main cause of instability (Capello, 1994; Kärrholm et al., 1999; Pekkarinen et al., 2000). The recoil properties appear determinant for the initial stability and the results from Paper III provide clinically relevant tools for a better control and conscious utilisation of the mechanical potential in it, either as an inert material guarantying little deformation over time or as an active component inducing a radial compressive pre-load on the implant.

At revision surgery, about 61 % of the femoral components are cemented, almost always with antibiotic cement (Furnes et al., 2004). While only about 7 % of primary operations in Norway use bone grafts either in the acetabulum or in the femur, almost 50 % of revisions use this technique and at least half of these in the femur. Pure re-cementation showed poor results compared to uncemented femoral stems with bone grafts or cemented stems with impacted morsellised bone (Lie et al., 2004). The use of cement in combination to morsellised bone

is indeed found to enhance the bone-cement locking thus improving the implant stability (Nelissen et al., 1995; Slooff et al., 1996).

3 Bone remodelling

During the second half of the 19^{th} century, much work was done on the study of how the mechanical environment influences bone growth, maintenance and degeneration (Roesler, 1987). The idea that bone shape is related to its function is usually attributed to Julius Wolff an anatomist and orthopaedic surgeon who observed that the trabecular structure of cancellous bone coincided with the stress trajectories (Wolff, 1892). This observation evolved to what is now known as Wolff's law stating that bone is formed as a mechanically optimal structure of maximal strength and minimal weight (Roesler, 1987).

To this view on bone as a solution of an optimisation problem, Rik Huiskes (2000) opposes the view by Wilhelm Roux (1881) according to whom formation and functional adaptation of bone results only from a self-organising process, regulated locally by cells and governed by mechanical stimuli.

Though modern computational methods (finite element analysis — FEA) confirm the coincidence of the trabecular architecture with stress trajectories, these are calculated in a continuum, which impairs the comparison with stress trajectories in a trabecular structure (Cowin, 1997). The similarity of trabecular bone and stress trajectories seems to be fortuitous and not causal (Huiskes, 2000).

3.1 The physiological processes

3.1.1 Load bearing and change in bone mass

Although bone modelling and remodelling may involve many factors such as gender, age or nutrition, they are mainly influenced in adults by calcium regulating hormones and functional load bearing (Lanyon, 1996). While physical exercise, such as training or normal weight bearing activities, increases bone mass (Courteix et al., 1998), deprivation of loading, as in micro-gravity, reduces it (Zerwekh et al., 1998). Menopausal women, for example, can retard bone loss associated to osteoporosis by exercising (Milliken et al., 2003).

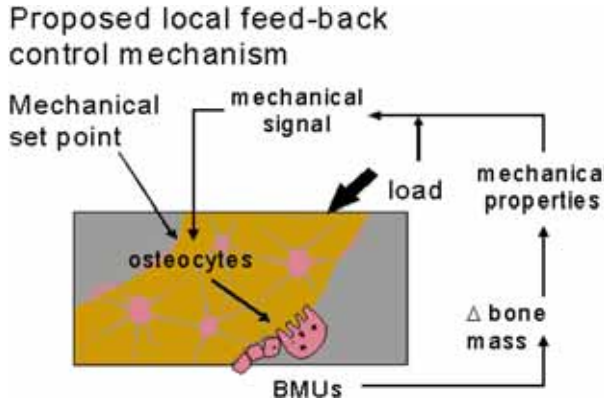

Figure 3: Regulatory process of the type suggested by Frost. This specific model was investigated by (Mullender and Huiskes, 1995). Figure reproduced from Huiskes (2000).

3.1.2 Cellular mechanisms

Following Roux's view on bone remodelling, Frost (Frost, 1988) proposed his "mechanostat"-theory in which local strains control bone remodelling (as a thermostat controls temperature). Though the complete mechanism still is not understood (Huiskes, 2000), there is a common agreement that osteocytes are the mechano-sensitive elements in bone (Klein-Nulend et al., 1995) commanding bone multi-cellular units (BMU) of osteoblasts and osteoclasts responsible for bone apposition and resorption respectively.

3.2 Modelling mechanically induced bone remodelling

Adaptive bone remodelling was formalised in a mathematical model by Cowin and Hegedus (1976) on adaptive elasticity. Soon thereafter, a comprehensive work by Rik Huiskes (1987) founded the computational simulation of bone remodelling in the particular case of a femoral cortex around an intramedullary prosthesis.

A concise remodelling scheme simulated changes in bone amount similar to changes measured in dogs (Weinans et al., 1992; Van Rietbergen et al., 1993).

The adaptive bone remodelling simulation theory is based on a site-specific formulation. The remodelling signal S is the strain energy per unit of mass (Carter, 1987). It regulates the bone mass m by attempting to normalise the signal to the same value as the pre-operative one. This model has been the core of continued investigations (Kerner et al., 1999) and is the one used in Paper III.

The rate of net bone turnover is expressed as a tri-linear function of the remodelling signal, the specific strain energy, expressed locally:

$$\frac{dm}{dt} = \tau A(\rho)[S - (1-s)S_{ref}] \qquad S < (1-s)S_{ref}$$

$$\frac{dm}{dt} = 0 \qquad (1-s)S_{ref} < S < (1+s)S_{ref}$$

$$\frac{dm}{dt} = \tau A(\rho)[S - (1+s)S_{ref}] \qquad S > (1+s)S_{ref}$$

In these equations, t is time, τ a time constant, $A(\rho)$ the free surface able to remodel as a function of the bone density ρ, S and S_{ref} the current and reference value of the specific strain energy and s is a threshold value defining a dead zone around the preoperative value. The maximum value for the bone density is set to 1.73 g/cm^3. The rate of net bone turnover can be split into external modelling: $\frac{dm}{dt} = \rho A \frac{dx}{dt}$ where x is a coordinate normal to the periosteum, and A is the surface of periosteum where the remodelling takes place, and an internal remodelling: $\frac{dm}{dt} = V \frac{d\rho}{dt}$ where V is the volume of bone where the change of density takes place. The surface function $A(\rho)$ is based on the theory by Martin (1972) according to which bone remodelling occurs only at free surfaces. He calculated the free trabecular surface per unit volume $a(\rho)$ as a function of the density assuming spherical pores. The relationship used by Weinans (1992) is closely approximated in Paper III by the following formula: $a(\rho) = 4\rho(1.73 - \rho)$ where the bone density ρ is in g/cm^3 and the surface density in mm^2/mm^3.

In the light of the considerations by Huiskes (2000) on the optimality of bone and paradigms in bone remodelling simulation, this model by Weinans, though not based on cellular activity, follows Roux's paradigm. It is not based on maximising strength and minimising weight but simply on local regulation of bone density and volume, governed by mechanical stimuli. However, its application to a continuum bypasses the concept of trabecular architecture itself. Considering rather the density distribution, Weinans' model fits fully Roux's understanding of the adaptation of bone.

An essential difference to be noted between this model and a cellular one proposed by Mullender and Huiskes (Mullender and Huiskes, 1995) is that the mechanical signal is a specific strain energy in the first case and a rate of strain energy density in the second. The adaptive stimulus is believed to be dynamic strains (Turner, 1998) and more specifically that it increases if the magnitude

or the frequency of the dynamic load increases (Turner et al., 1995). Neither Weinans nor Van Rietbergen comment on this aspect in their articles, though the suggestions of dynamic loads as stimuli of bone adaptation had been published earlier (Lisková and Hert, 1971; Lanyon and Rubin, 1984).

4 Computational and imagery techniques

4.1 The finite element method in biomechanics

4.1.1 The finite element method (FEM)

The FEM is a general mathematical method to solve numerically partial derivative equations on spatial domains. In solid mechanics it allows extrapolating stresses through solids based on knowledge of external forces, material properties and geometry of the considered body. The global domain is divided into many small ones: finite elements, together forming a mesh of the global domain. The basic hypothesis is to assume the shape of the displacement field within each element and that the displacement field is described by the values at special points of the elements: the nodes. Forces and displacements for an element are related by an elementary stiffness matrix $\mathbf{K^e}$ by integrating the assumed displacement field into the principle of virtual powers. By putting the $\mathbf{K^e}$'s together according to the nodes shared by two neighbour elements, they form the stiffness matrix of the whole structure $\mathbf{K}$, relating nodal displacements to nodal forces by $\mathbf{F} = \mathbf{K}\boldsymbol{\delta}$, where $\mathbf{F}$ is the vector of nodal forces and $\boldsymbol{\delta}$ the vector of nodal displacement. For all nodes except the ones on which forces are applied, the nodal force is zero by principle of equilibrium. Strains are derived from displacements and through material properties, stresses can be calculated.

4.1.2 Applications to tissue mechanics

Huiskes and Chao (1983) traced the first application of the FEM to orthopaedics back to 1972 (Brekelmans). Three main fields of application of the FEM can be discerned: design and pre-clinical analysis of prostheses, acquisition of knowledge about musculoskeletal structures, and study of the adaptive behaviour of tissues (Prendergast, 1997). Because of the complex and curved shapes of the musculoskeletal structures to be analysed, the generation of a mesh requires special techniques. Geometries are increasingly generated using computer tomography (CT) scanning either by adjusting nodes on the contours or by directly

converting the voxels into finite elements (Merz et al., 1996). In Paper III, cortical bone contours were extracted based on a critical CT density (Aamodt et al., 1999).

The analysis by Brekelmans et al. (1972) was also the first on a whole bone, the femur and established the determinant role of abductor muscles for stresses in the diaphysis. Hip replacement was first analysed in a larger (5000 nodes) three dimensional (3D) model by Rohlmann et al. (1983), including implant, cement and bone. Strain gauge measurements on the contralateral bone were performed for validation. They found "a reasonable agreement". Many FE analyses report studies of known designs (Yettram, 1989; Keaveny and Bartel, 1993) but it was Huiskes and Vroemen (1986) who developed systematic prediction of maximum normal and shear stresses at implant interfaces as preclinical evaluation.

Studying cylindrical components, Harrigan et al. (1991) showed that interface gaps of less than 20 μm between bone and implant can substantially change the contact stress distribution. A 2D analysis of uncemented arthroplasty showed that even a low friction between bone and implant could reduce interfacial micromotions (Kuiper and Huiskes, 1996). Limiting the porous coating for bone ingrowth in uncemented implant to the proximal region is also predicted to provide a more physiological stress transfer (Tensi et al., 1989). Interfacial micromotions often lead to growth of a fibrous layer between the implant and the bone. Modelled as linear elastic it reproduced in simulation the drastic effect on the load transfer pattern (Brown et al., 1988). Another modelling of the fibrous layer as a highly compliant material with little resistance against tension and shear (Weinans et al., 1990) illustrated the drastic change in load transfer mainly due to tensile loosening and slip at the interface.

Further modelling of hip arthroplasty implies time-dependent adaptive behaviour and is reported in the section on bone remodelling.

4.2 Dual energy x-ray absorptiometry (DEXA)

4.2.1 Basic principles

Absorptiometry is a quantitative method to determine the amount of bone mineral. It measures, strictly speaking, the amount of calcium hydroxyapatite per unit volume of the tissue examined. Single x-ray absorptiometry necessitates a constant thickness of soft tissue over the area of interest in order to subtract its absorption. The body part is therefore placed in a soft tissue equivalent

material (usually water). This requirement makes the technique little suitable for body parts as the spine or the hip.

Dual energy x-ray absorptiometry uses a filter to produce two narrow energy peaks. The different attenuation coefficients for the different energies eliminate the need for constant soft tissue thickness. The attenuation for x-rays penetrating tissue is: $N = N_0 e^{-\mu x}$, where N is the number of transmitted photons, N_0 is the number of incident photons, μ is the attenuation coefficient and x the thickness of tissue. Using 1 and 2 subscripts for the two energy levels and superscripts S and H for soft and hard tissue, we obtain for each pixel:

$$N_1 = N_0 \exp\left(-\mu_1^S x^S - \mu_1^H x^H\right) \quad (1)$$

$$N_2 = N_0 \exp\left(-\mu_2^S x^S - \mu_2^H x^H\right) \quad (2)$$

with known attenuation coefficients for both energies in soft tissue and for hydroxyapatite, the equivalent thickness of bone mineral can be calculated at each pixel, independently of the soft tissue thickness. This technique is the most precise to measure bone mineral density.

4.2.2 Gruen zones

The method described above allows quantification of the amount of bone mineral within a pixel of the projection image and with a known resolution. This gives a bone mineral density per unit area (BMD), usually given in g/cm^2. Edge detection programs allow differentiating bone tissue from soft tissue and/or metallic implant when DEXAs of the operated patient are taken. The projected bone area thus calculated is a useful quantity to monitor changes in bone geometry. These can be due to external modelling following insertion of a femoral implant or to the natural aging process showing a thinning of the cortical bone and widening of the medullary canal (Noble et al., 1988). Finally, combining the bone density data with the projected bone area, the bone mineral content (BMC) can be calculated providing a global measure of the bone stock independently of porosity or volume consideration. The three quantities BMC, projected bone area and BMD and their interrelations are the kernel of Paper I to analyse structural changes in bone after insertion of a femoral implant.

Antero-posterior (frontal) x-rays of the proximal femur with inserted implant are often divided into seven zones called Gruen zones. Their definition is based on anatomic features (trochanter minor, tip of the implant) and is therefore reproducible between x-rays. They start proximally laterally with zone 1, move distally along the lateral side to reach zone 4 under the implant, and go

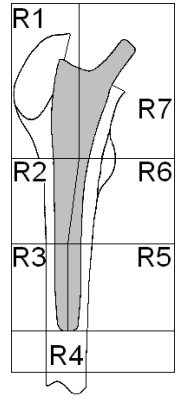

Figure 4: The seven Gruen zones, denoted from R1 to R7, are represented on a right upper femur with inserted implant.

proximally along the medial side to end at zone 7 at the calcar zone. DEXA results are usually summed up within the Gruen zones excluding the implant and reported as seven BMC, projected bone areas and BMD, together with an average for the union of the seven zones. The precision of the method is estimated to 3 % (Cohen and Rushton, 1995) and patient position causes variations of 5 % within 15° internal and external rotation (Mortimer et al., 1996).

4.3 Computer tomography

This technique of imagery was introduced in 1972 by G.N. Hounsfield. The essential idea behind computer tomography (CT) is that the internal structure of an object can be reconstructed from multiple projections of the object (Curry et al., 1990). A pencil of x-ray hits the object and the transmitted radiation is registered by a detector from multiple angles in a plane, a tomographic slice. The gathered data are treated by a computer to reconstruct the cross-sectional structure of the object.

The theoretical problem to be solved can be outlined as follows. The tissue is divided into a matrix of voxels of attenuation coefficient μ_{ij} and of width x. Using two perpendicular pencils of x-rays along the directions of the matrix

of voxels and writing the equation for the transmitted fraction of the incident photons, we obtain a large linear system of equations of the following type:

$$N_{i\bullet} = N_0 \exp\left(-x \sum_j \mu_{ij}\right) \quad (3)$$

$$N_{\bullet j} = N_0 \exp\left(-x \sum_i \mu_{ij}\right) \quad (4)$$

where the first type of equations accounts for the rows and the second type for the columns. In reality artefacts in so-called star-pattern appear due to the few projections. Therefore, many more projection angles are added to improve image quality but the principle remains identical.

Based on this method, the resulting cross section is a table of attenuation coefficients but in practice they are converted to CT numbers, also called Hounsfield units, to present the image on a large gray scale:

$$CTnumber_p = K \frac{\mu_p - \mu_w}{\mu_w}$$

where mu_p is the attenuation of the current pixel, μ_w the attenuation of water and K a magnification constant. Thus water will have a CT number of zero and air (assumed not to interact with x-rays) a CT number of $-K$. It is based on these values that bone densities of bone are derived in Paper II for inhomogeneous attribution of mechanical properties.

CTs are usually taken in series spaced in the longitudinal direction (perpendicular to the cross section) with the slice distance. The depth of the voxels is the slice thickness. If the slice distance is equal to the slice thickness, the CTs are taken edge to edge and the whole volume is described. If the distance is larger than the thickness, some volume between the slices will not be described; if the distance is less than the thickness, the slices overlap and the information will be redundant. The slice thickness introduces a certain blurring studied by Hangartner and Shah (2003). Objects with inhomogeneities or boundaries that do not extend at right angles to the measurement plane are inaccurately represented. The calculated attenuation coefficient for a voxel is a weighted average of all materials in the voxel. Thus, an oblique bone boundary appears both wider but also, as its CT number is averaged with soft tissue, it appears less dense. The CTs used in Paper II were taken every 5 mm edge to edge and the blurring effect due to the voxel depth was a problem in the proximal tapered

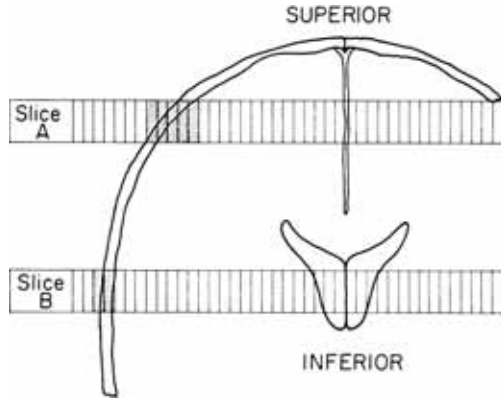

Figure 5: The effect of object boundaries that do not extend at right angles to the measurement plane. The slice B will have a correct representation of the skull while the slice A will show a wider and less sharp cranial bone as the bone density is averaged with air or soft tissue. Reproduced from (Curry, Thomas S, III. Dowdey, James E. Murry, Robert C, JR., 1990).

area of the femur. This motivated the use of cortical density estimated distally where the femur is straight.

Summary of papers

Paper I: A quantitative and qualitative analysis of bone remodelling around custom uncemented femoral stems: a five-year DEXA follow-up.
Five years of postoperative bone remodelling recorded by DEXA are analysed to establish the relationship between preoperative bone stock and relative change of bone amount after five years. A geometric interpretation of DEXA measurements brings light on the changes of bone structure at a macroscopic level during the same five-year remodelling period.
Published in Clinical Biomechanics *2005,* ***20****(3):277-282.*
Part of this work was presented at the World Congress on Medical Physics and Biomedical Engineering, Sydney, August 2003.

Paper II: Comparison of patient-specific bone remodelling simulation and five-year in vivo DEXA measurements.
An established strain-adaptive bone remodelling model is quantitatively tested by running the simulations on patient-specific models and comparing locally their results over time to the DEXA measurements in the corresponding living patients over five years. The results have a good predictive value through a regression.
Submitted, Journal of Biomechanics.
Part of this work has been presented at the 14th congress of the European Orthopaedic Research Society, Amsterdam, November 2004.

Paper III: Viscoelastic modelling of impacted morsellised bone accurately describes unloading behaviour.
A linear viscoelastic solid model is applied to impacted morsellised bone relaxing after confined compression. Three clinically relevant quantities are derived from the immediate material properties and used to discriminate the influence of varying pre-treatments for the morsellised bone.
To be submitted, Journal of Biomechanics.
Part of this work was presented at the congress of the Nordic Orthopaedic Society, Reykjavik, June 2004.

Paper IV: Morsellised bone under compression and torsion in femoral canal-like cavity. Comparison of finite element simulations and experimental data.

The response of impacted morsellised bone to axial compression and torsion is tested in a cavity mimicking the femoral canal. A linear viscoelastic solid model is implemented in a finite element model of the experiment to validate or invalidate the material model.
In preparation for publication.

References

Aamodt, A., Kvistad, K.A., Andersen, E., Lund-Larsen, J., Eine, J., Benum, P., Husby, O.S., 1999. Determination of Hounsfield value for CT-based design of custom femoral stems. *J Bone Joint Surg Br* 81, 143-147.

Bourne, R.B., Rorabeck, C.H., 1998. A critical look at cementless stems. Taper designs and when to use alternatives. *Clin Orthop* 355, 212-223.

Bourne, R.B., Rorabeck, C.H., Laupacis, A., Feeny, D., Tugwell, P.S., Wong, C., Bullas, R., 1995. Total hip replacement: the case for noncemented femoral fixation because of age. *Can J Surg* 38 Suppl 1, S61-S66.

Brekelmans, W.A., Poort, H.W., Slooff, T.J., 1972. A new method to analyse the mechanical behaviour of skeletal parts. *Acta Orthop Scand* 43, 301-317.

Brewster, N.T., Gillespie, W.J., Howie, C.R., Madabhushi, S.P., Usmani, A.S., Fairbairn, D.R., 1999. Mechanical considerations in impaction bone grafting. *J Bone Joint Surg Br* 81, 118-124.

Brown, T.D., Pedersen, D.R., Radin, E.L., Rose, R.M., 1988. Global mechanical consequences of reduced cement/bone coupling rigidity in proximal femoral arthroplasty: a three-dimensional finite element analysis. *J Biomech* 21, 115-129.

Bugbee, W.D., Culpepper, W.J.2., Engh, C.A.J., Engh, C.A.S., 1997. Long-term clinical consequences of stress-shielding after total hip arthroplasty without cement. *J Bone Joint Surg Am* 79, 1007-1012.

Callaghan, J.J., Forest, E.E., Sporer, S.M., Goetz, D.D., Johnston, R.C., 1997. Total hip arthroplasty in the young adult. *Clin Orthop* 344, 257-262.

Capello, W.N., 1994. Impaction grafting plus cement for femoral component fixation in revision hip arthroplasty. *Orthopedics* 17, 878-879.

Carter, D.R., 1987. Mechanical loading history and skeletal biology. *J Biomech* 20, 1095-1109.

Cohen, B., Rushton, N., 1995. Accuracy of DEXA measurement of bone mineral density after total hip arthroplasty. *J Bone Joint Surg Br* 77, 479-483.

Courteix, D., Lespessailles, E., Peres, S.L., Obert, P., Germain, P., Benhamou, C.L., 1998. Effect of physical training on bone mineral density in prepubertal girls: a comparative study between impact-loading and non-impact-loading sports. *Osteoporos Int* 8, 152-158.

Cowin, S.C., 1993. Bone stress adaptation models. *J Biomech Eng* 115, 528-533.

Cowin, S.C., 1997. The false premise of Wolff's law. *Forma* 12, 247-262.

Cowin, S.C., Hegedus, D.H., 1976. Bone remodelling I: theory of adaptive elasticity. *J Elast* 6, 313-326.

Crowninshield, R.D., Maloney, W.J., Wentz, D.H., Levine, D.L., 2004. The role of proximal femoral support in stress development within hip prostheses. *Clin Orthop* 420, 176-180.

Currey, J.D., 1984. In *The mechanical adaptations of bones*. Princeton University Press, Princeton, New Jersey.

Curry, Thomas S. III, Dowdey, James E., Murry, Robert C. JR., 1990. In *Christensen's Physics of Diagnostic Radiology*. Lea & Febiger, Philadelphia.

de Ricqles, A., Meunier, F.J., Castanet, J., Francillon-Vieillot, H., , 1991. Comparative microstructure of bone. In *Bone Volume 3*. Hall, B.K.pp 1-78. CRC Press, Boca Raton.

Dohmae, Y., Bechtold, J.E., Sherman, R.E., Puno, R.M., Gustilo, R.B., 1988. Reduction in cement-bone interface shear strength between primary and revision arthroplasty. *Clin Orthop* 236, 214-220.

Edvardsen, P., 1989. In *Ortopedisk kirurgi*. Cappelens Forlag.

Engh, C.A., McGovern, T.F., Bobyn, J.D., Harris, W.H., 1992. A quantitative evaluation of periprosthetic bone-remodeling after cementless total hip arthroplasty. *J Bone Joint Surg Am* 74, 1009-1020.

Eriksen, E.F., Vesterby, A., Kassem, M., Melsen, F., Mosekilde, L., , 1993. Bone remodeling and bone structure. In *Physiology and pharmacology of bone*. Born, G.V.R., Cuatrecasas, P., Herken, H., Melmon, K.pp 67-109. Springer Verlag, Berlin.

Frost, H.M., 1988. Vital biomechanics: proposed general concepts for skeletal adaptations to mechanical usage. *Calcif Tissue Int* 42, 145-156.

Furnes, O., Havelin, L.I., Espehaug, B., 2004. In *The Norwegian arthroplasty register. Annual report 2004*. Haukeland university hospital, Bergen, Norway: 2004.

Gie, G.A., Linder, L., Ling, R.S., Simon, J.P., Slooff, T.J., Timperley, A.J., 1993. Impacted cancellous allografts and cement for revision total hip arthroplasty. *J Bone Joint Surg Br* 75, 14-21.

Giesen, E.B., Lamerigts, N.M., Verdonschot, N., Buma, P., Schreurs, B.W., Huiskes, R., 1999. Mechanical characteristics of impacted morsellised bone grafts used in revision of total hip arthroplasty. *J Bone Joint Surg Br* 81, 1052-1057.

Giraud-Guille, M.M., 1988. Twisted plywood architecture of collagen fibrils in human compact bone osteons. *Calcif Tissue Int* 42, 167-180.

Hangartner, T.N., Shah, D., , 2003. Modeling of blurring due to finite slice width in computed tomography. In *Proceedings of the World Congress on*

Medical Physics and Biomedical Engineering [CD-ROM]. Anonymous. pp Paper No 1652. , Sydney, Australia.

Harrigan, T.P., Harris, W.H., 1991. A finite element study of the effect of diametral interface gaps on the contact areas and pressures in uncemented cylindrical femoral total hip components. *J Biomech* 24, 87-91.

Hooten, J.P., Engh, C.A., Heekin, R.D., Vinh, T.N., 1996. Structural bulk allografts in acetabular reconstruction. Analysis of two grafts retrieved at post-mortem. *J Bone Joint Surg Br* 78, 270-275.

Huiskes, R., 1987. Finite element analysis of acetabular reconstruction. Noncemented threaded cups. *Acta Orthop Scand* 58, 620-625.

Huiskes, R., 1990. The various stress patterns of press-fit, ingrown, and cemented femoral stems. *Clin Orthop* 261, 27-38.

Huiskes, R., 1993. Stress shielding and bone resorption in THA: clinical versus computer-simulation studies. *Acta Orthop Belg* 59 Suppl 1, 118-129.

Huiskes, R., 2000. If bone is the answer, then what is the question? *J Anat* 197, 145-156.

Huiskes, R., Chao, E.Y., 1983. A survey of finite element analysis in orthopedic biomechanics: the first decade. *J Biomech* 16, 385-409.

Huiskes, R., Vroemen, W., 1986. A standardized finite element model for routine comparative evaluations of femoral hip prostheses. *Acta Orthop Belg* 52, 258-261.

Huiskes, R., Weinans, H., van Rietbergen, B., 1992. The relationship between stress shielding and bone resorption around total hip stems and the effects of flexible materials. *Clin Orthop* 274, 124-134.

Jasty, M., Bragdon, C., Burke, D., O'Connor, D., Lowenstein, J., Harris, W.H., 1997. In vivo skeletal responses to porous-surfaced implants subjected to small induced motions. *J Bone Joint Surg Am* 79, 707-714.

Kärrholm, J., Hultmark, P., Carlsson, L., Malchau, H., 1999. Subsidence of a non-polished stem in revisions of the hip using impaction allograft. Evaluation with radiostereometry and dual-energy X-ray absorptiometry. *J Bone Joint Surg Br* 81, 135-142.

Keaveny, T.M., Bartel, D.L., 1993. Load transfer with the Austin Moore cementless hip prosthesis. *J Orthop Res* 11, 272-284.

Kerner, J., Huiskes, R., van Lenthe, G.H., Weinans, H., van Rietbergen, B., Engh, C.A., Amis, A.A., 1999. Correlation between pre-operative periprosthetic bone density and post-operative bone loss in THA can be explained by strain-adaptive remodelling. *J Biomech* 32, 695-703.

Kirkeby, O.J., Berg-Larsen, T., 1991. Regional blood flow and strontium-85 incorporation rate in the rat hindlimb skeleton. *J Orthop Res* 9, 862-868.

Kirkeby, O.J., Pinholt, E., Larsen, T.B., 1992. Fresh, frozen, or decalcified bone grafts: a study of early vascularisation and mineralisation of allogeneic and syngeneic bone grafts in rats. *Scand J Plast Reconstr Surg Hand Surg* 26, 141-145.

Klein-Nulend, J., van der Plas, A., Semeins, C.M., Ajubi, N.E., Frangos, J.A., Nijweide, P.J., Burger, E.H., 1995. Sensitivity of osteocytes to biomechanical stress in vitro. *FASEB J* 9, 441-445.

Kobayashi, S., Eftekhar, N.S., Terayama, K., Joshi, R.P., 1997. Comparative study of total hip arthroplasty between younger and older patients. *Clin Orthop* 339, 140-151.

Kuiper, J.H., Huiskes, R., 1996. Friction and stem stiffness affect dynamic interface motion in total hip replacement. *J Orthop Res* 14, 36-43.

Lanyon, L.E., 1996. Using functional loading to influence bone mass and architecture: objectives, mechanisms, and relationship with estrogen of the mechanically adaptive process in bone. *Bone* 18, 37S-43S.

Lanyon, L.E., Rubin, C.T., 1984. Static vs dynamic loads as an influence on bone remodelling. *J Biomech* 17, 897-905.

Lie, S.A., Havelin, L.I., Furnes, O.N., Engesaeter, L.B., Vollset, S.E., 2004. Failure rates for 4762 revision total hip arthroplasties in the Norwegian Arthroplasty Register. *J Bone Joint Surg Br* 86, 504-509.

Lisková, M., Hert, J., 1971. Reaction of bone to mechanical stimuli. 2. Periosteal and endosteal reaction of tibial diaphysis in rabbit to intermittent loading. *Folia Morphol (Praha)* 19, 301-317.

Malkani, A.L., Voor, M.J., Fee, K.A., Bates, C.S., 1996. Femoral component revision using impacted morsellised cancellous graft. A biomechanical study of implant stability. *J Bone Joint Surg Br* 78, 973-978.

Martin, R.B., 1972. The effects of geometric feedback in the development of osteoporosis. *J Biomech* 5, 447-455.

Merz, B., Niederer, P., Müller, R., Rüegsegger, P., 1996. Automated finite element analysis of excised human femora based on precision -QCT. *J Biomech Eng* 118, 387-390.

Milliken, L.A., Going, S.B., Houtkooper, L.B., Flint-Wagner, H.G., Figueroa, A., Metcalfe, L.L., Blew, R.M., Sharp, S.C., Lohman, T.G., 2003. Effects of exercise training on bone remodeling, insulin-like growth factors, and bone mineral density in postmenopausal women with and without hormone replacement therapy. *Calcif Tissue Int* 72, 478-484.

Mortimer, E.S., Rosenthall, L., Paterson, I., Bobyn, J.D., 1996. Effect of rotation on periprosthetic bone mineral measurements in a hip phantom. *Clin Orthop* 324, 269-274.

Mullender, M.G., Huiskes, R., 1995. Proposal for the regulatory mechanism of Wolff's law. *J Orthop Res* 13, 503-512.

Naidu, S.H., Cuckler, J.M., Burkholder, T., Ducheyne, P., 1996. Initial stability of a modular uncemented, porous-coated femoral stem: a mechanical study. *Am J Orthop* 25, 829-834.

Nelissen, R.G., Bauer, T.W., Weidenhielm, L.R., LeGolvan, D.P., Mikhail, W.E., 1995. Revision hip arthroplasty with the use of cement and impaction grafting. Histological analysis of four cases. *J Bone Joint Surg Am* 77, 412-422.

Pekkarinen, J., Alho, A., Lepistö, J., Ylikoski, M., Ylinen, P., Paavilainen, T., 2000. Impaction bone grafting in revision hip surgery. A high incidence of complications. *J Bone Joint Surg Br* 82, 103-107.

Prendergast, P.J., 1997. Finite element models in tissue mechanics and orthopaedic implant design. *Clin Biomech (Bristol, Avon)* 12, 343-366.

Rauber, A.A., 1876. In *Über Elastizität und Festigkeit der Knochen.* Wilhelm Engelmann, Leipzig.

Reilly, D.T., Burstein, A.H., 1975. The elastic and ultimate properties of compact bone tissue. *J Biomech* 8, 393-405.

Roesler, H., 1987. The history of some fundamental concepts in bone biomechanics. *J Biomech* 20, 1025-1034.

Rohlmann, A., Mössner, U., Bergmann, G., Kölbel, R., 1983. Finite-element-analysis and experimental investigation in a femur with hip endoprosthesis. *J Biomech* 16, 727-742.

Roux, W., 1881. In *Der Kampf der Teile im Organismus.* Springer, Berlin.

Sambrook, P., , 2001. Bone structure and function in normal and disease states. In *The musculoskeletal system. Basic science and clinical conditions.* Sambrook, P., Schrieber, L., Taylor, T., Ellis, A.pp 67-84. Churchill Livingstone, Edinburgh.

Schneider, R., 1989. In *Total prosthetic replacement of the hip.* Hans Huber Publishers, Toronto.

Slooff, T.J., Buma, P., Schreurs, B.W., Schimmel, J.W., Huiskes, R., Gardeniers, J., 1996. Acetabular and femoral reconstruction with impacted graft and cement. *Clin Orthop* 324, 108-115.

Slooff, T.J., Huiskes, R., van Horn, J., Lemmens, A.J., 1984. Bone grafting in total hip replacement for acetabular protrusion. *Acta Orthop Scand* 55, 593-596.

Solheim, E., Pinholt, E.M., Talsnes, O., Larsen, T.B., Kirkeby, O.J., 2001. Revascularisation of fresh compared with demineralised bone grafts in rats. *Scand J Plast Reconstr Surg Hand Surg* 35, 113-116.

Steen Jensen, J., , 1986. Regional ortopedi. Hofte. In *Ortopædisk kirurgi.* Sneppen, O.pp 332-357. Foreningen af Danske Lægestuderendes Forlag, Copenhagen.

Tensi, H.M., Gese, H., Ascherl, R., 1989. Non-linear three-dimensional finite element analysis of a cementless hip endoprosthesis. *Proc Inst Mech Eng [H]* 203, 215-222.

Turner, C.H., 1998. Three rules for bone adaptation to mechanical stimuli. *Bone* 23, 399-407.

Turner, C.H., Owan, I., Takano, Y., 1995. Mechanotransduction in bone: role of strain rate. *Am J Physiol* 269, E438-E442.

Ullmark, G., Nilsson, O., 1999. Impacted corticocancellous allografts: recoil and strength. *J Arthroplasty* 14, 1019-1023.

Van Buskirk, W.C., Ashman, R.B., , 1981. The elastic moduli of bone. In *Mechanical properties of bone AMD Vol.45.* Cowin, S.C.American Society of Mechanical engineers, New York.

Van Rietbergen, B., Huiskes, R., Weinans, H., Sumner, D.R., Turner, T.M., Galante, J.O., 1993. ESB Research Award 1992. The mechanism of bone remodeling and resorption around press-fitted THA stems. *J Biomech* 26, 369-382.

Van Rietbergen, B., Odgaard, A., Kabel, J., Huiskes, R., 1996. Direct mechanics assessment of elastic symmetries and properties of trabecular bone architecture. *J Biomech* 29, 1653-1657.

Voor, M.J., White, J.E., Grieshaber, J.E., Malkani, A.L., Ullrich, C.R., 2004. Impacted morselized cancellous bone: mechanical effects of defatting and augmentation with fine hydroxyapatite particles. *J Biomech* 37, 1233-1239.

Weinans, H., Huiskes, R., Grootenboer, H.J., 1990. Trends of mechanical consequences and modeling of a fibrous membrane around femoral hip prostheses. *J Biomech* 23, 991-1000.

Weinans, H., Huiskes, R., Grootenboer, H.J., 1992. Effects of material properties of femoral hip components on bone remodeling. *J Orthop Res* 10, 845-853.

Witsø, E., Persen, L., Løseth, K., Bergh, K., 1999. Adsorption and release of antibiotics from morselized cancellous bone. In vitro studies of 8 antibiotics. *Acta Orthop Scand* 70, 298-304.

Wolff, J., 1892. In *Das Gesetz der Transformation der Knochen.* A. Hirchwild., Berlin.

Yettram, A.L., 1989. Effect of interface conditions on the behaviour of a Freeman hip endoprosthesis. *J Biomed Eng* 11, 520-524.

Zerwekh, J.E., Ruml, L.A., Gottschalk, F., Pak, C.Y., 1998. The effects of twelve weeks of bed rest on bone histology, biochemical markers of bone turnover, and calcium homeostasis in eleven normal subjects. *J Bone Miner Res* 13, 1594-1601.

A quantitative and qualitative analysis of bone remodelling around custom uncemented femoral stems: a five year DEXA follow-up

Sébastien Muller[a,b], Fridtjov Irgens[a], Arild Aamodt[b]

[a] Faculty of Engineering Science and Technology, Department of Structural Engineering, Norwegian University of Science and Technology, Trondheim, Norway

[b] Norwegian Orthopaedic Implant Research Unit, St Olavs Hospital, MTFS, Olav Kyrresgate 3, 7489 Trondheim, Norway

Abstract

Background. After total hip replacement bone remodelling is determinant for the implant survival. This study asked whether the immediate postoperative amount and distribution of bone can predict the changes in bone amount and distribution after five years in the case of younger patients with custom uncemented implant.

Methods. We investigated 17 hips with a mean follow-up of 5.1 years. The average patient age at follow-up was 48.5 years. We used immediate postoperative and five-year dual energy X-ray absorptiometry measurements of bone mineral content, density, and projected bone area in seven local zones forming a partition of the upper femur. A correlation was sought between the preoperative variables and the five-year variation. Qualitative bone remodelling was analysed considering each local zone in a density-area plane. Based on geometrical considerations, we introduced an *index of structural remodelling*, which expresses the preponderance of internal remodelling against external modelling.

Findings. The bone mineral content at operation correlated significantly with its relative decrease locally laterally mid-proximally and medially ($P < 0.01$), distally, and globally for the femur ($P < 0.05$). For the bone mineral density, the correlation was significant distally, medially and globally ($P < 0.05$). The projected bone area shows only significant correlation laterally mid-proximally ($P < 0.01$). The index of structural remodelling was significantly positive ($P < 0.01$) in all local zones and was independent of the initial bone amount and structure ($P > 0.1$).

Interpretation. High bone mineral content at operation correlates significantly with periprosthetic bone loss after five years in younger patients with cementless custom femoral implant. Independently of the net bone mineral content balance, external modelling is stronger than internal remodelling in all local zones.

Published in *Clinical Biomechanics* 2005, **20**(3):277-282.

1 Introduction

The qualitative aspect of periprosthetic bone remodelling has been extensively reported in the literature. Follow-up studies for most implant types describe qualitatively the frequency and distribution in gain or loss of bone mass, and the presence of radiolucencies, or osteolytic lesions (Clohisy and Harris, 1999; Eingartner et al., 2000; Keisu et al., 2001).

A number of studies use dual energy X-ray absorptiometry (DEXA) to monitor changes in bone mineral content (BMC), bone mineral density (BMD), and projected bone area after insertion of different implants (Engh et al., 1992; Kilgus et al., 1993). Cohen and Rushton (1995) showed, using two different implant types, that the in vivo mean coefficient of variation of the BMD varied between 2.7 and 3.4 % for repeated measurements in the same conditions. The reliability of DEXA for the measurement of changes in bone mass around prostheses has also been documented by others (Larnach et al., 1992; Kröger et al., 1996). Primarily, the measurement error follows from the variations in the position of the patient during scanning. Mortimer (1996) showed that the BMD and the BMC varied within 5 % between 15° internal and 15° external rotation.

Sychterz and Engh (1996) reported a positive correlation between initially low BMC and high postoperative bone loss. However, these results are based on DEXA measurements of BMC in bones retrieved from elderly patients post mortem previously equipped with a straight extensively coated endoprosthesis. A recent in vivo study (Rahmy et al., 2004) reported the same relation based on measurements of BMD.

Young patients show a different remodelling activity both at the cellular (Groessner-Schreiber et al., 1992) and at the macroscopic level (Brockstedt et al., 1991). Their more active lifestyle, often mentioned as a cause of implant loosening (Dorr et al., 1997), also represents increased loads on the femur and thus a stimulus for gain in bone mass. Together these findings suggest that younger patients might have a different remodelling pattern after the insertion of orthopaedic implants.

Follow-up studies of bone remodelling only report the evolution of BMC or BMD as a function of time (Massari et al., 1995; Kröger et al., 1996; Georges et al., 2002). These data reflect only either the total remodelling or the internal remodelling and these concepts are often confused. In this paper, we call internal remodelling, the reorganisation of cancellous bone resulting in changes of bone density, while we call external modelling processes occurring at the external surface of bone resulting in geometrical changes. Total remodelling sometimes simply called remodelling denotes then both processes. In addition to the redis-

tribution of bone mineral content (total remodelling) also the external modelling or the change in femoral shape (surface modelling) is of great interest in order to understand the adjustment of bone to a new mechanical environment.

Therefore, the objective of the present study was twofold. First, we examined whether a predictive relationship could be established between pre-operative bone quality and bone remodelling in order to help identifying patients at risk for increased bone loss and, secondly, we mapped changes in bone structure by comparing external modelling with internal remodelling. For this purpose we hypothesized that BMC, projected bone area, and BMD could be quantitative predictors of bone remodelling in the proximal femur in younger patients after insertion of a custom implant, then we tried to describe changes in the bone structure based on DEXA output.

2 Methods

2.1 Patients.

Nine men and seven women (17 hips) were operated between June 1997 and June 1998 with a custom uncemented femoral implant (*Unique*, Scandinavian Customized Prostheses, Trondheim, Norway). The mean patient age at operation was 43.4 years (ranging from 20 to 59 years) and the mean follow-up time was 5.1 years (ranging from 4.6 to 5.6 years). Two experienced surgeons performed all hip replacements. All measurements were performed with one DEXA machine (Hologic QDR4500, Bedford, USA) and by one experienced operator. The patients' bone mineral content, projected bone area, and bone mineral density were measured during the first postoperative week and after five years. The rotation of the leg during the DEXA examination was maintained constant by a specially designed cushion.

Two models were used to analyse bone remodelling. A quantitative model was applied to establish a predictive relationship between pre-operative bone stock and bone remodelling, and a qualitative model was developed to analyse the changes in the bone structure.

2.2 Quantitative model.

The parameters used for the correlation analysis were BMC, projected bone area, and BMD (denoted C, A, and D respectively) at operation and after five years. They were measured locally for each of the seven Gruen zones in the

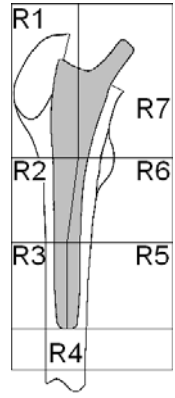

Figure 1: The seven Gruen zones R1 to R7 and their combination denoted *global*.

frontal plane (Figure 1) and for all zones combined (hereafter called *global*). The Gruen zones are defined manually following anatomical features and stored in a template to be used for the following examinations. The method is described only for BMC, as projected bone area and BMD follow exactly the same procedure.

If one bone has more material than another pre-operatively, then the same absolute amount of gain or loss will be more significant for the bone with the lower value of BMC. We need to scale bone gain or loss with respect to the initial BMC. This is easily done using the relative change of BMC $\frac{C}{C_0}$ where C_0 is the value of C at operation. A correlation was calculated between: $\frac{C}{C_0}$ and a dimensionless BMC at operation: $\frac{C}{\langle C_0 \rangle}$, where $\langle C_0 \rangle$ is the average C_0 in the study population. A linear regression was then calculated between the two variables. The continued use of dimensionless quantities ensures better numerical precision and allows a direct interpretation of the coefficients of the linear regressions performed.

2.3 Qualitative model.

The separate evolutions of BMC, projected bone area, and BMD as a function of time do not allow easy comparison of relative changes. This is much easier done by plotting BMD and projected bone area along a horizontal and a vertical axis respectively (Figure 2). Each joint measurement of BMD and projected bone area can be represented by a single point on the plane. The observations can then form a path whose shape brings a new light on the interpretation of the remodelling process. The state of the bone at any time is represented by a point (D, A). The surface of the rectangle below and to the left in the density-area plane is the product of the projected bone area by the bone mineral density: $D \times A = C$, so the surface of the rectangle is equal to the BMC. The shape of this *bone mineral content rectangle* characterizes the way bone mass is stored in the bone. We call it *bone storage profile*: a big and porous bone has a big projected bone area and a low density. It is represented by a high and narrow rectangle. On the other hand, a small and dense bone (small projected bone area and high density) is represented by a low and wide rectangle. The relative height and width of the rectangle shows the extent to which the bone is *stored as volume* or *stored as density*. Changes in the shape of the rectangle will reflect the relative amount of internal remodelling and surface modelling (density and projected bone area respectively). Changes in surface are equal to the change in bone mass.

To analyse the changes of quality, and not quantity, of the bone storage profile, we need to compare rectangle shapes and not areas. For this purpose we introduce the angle φ formed by the diagonal of the rectangle and the density axis. For example at operation time t_0: $\tan\varphi_0 = \frac{A_0}{D_0}$, and at time t: $\tan\varphi = \frac{A}{D}$. Thus to compare the bone storage profile at time t to the one at t_0, we simply form $\Delta\varphi = \varphi - \varphi_0$. The average angle change $\Delta\varphi$ is computed in each Gruen zone and at the global level. $\Delta\varphi$ is a direct and obvious geometrical comparison tool but its physical meaning remains difficult to interpret. Therefore we propose the following evaluation procedure.

We want to decompose the remodelling processes that bring the initial point (D_0, A_0) to the point (D, A). Firstly we scale the initial rectangle equally along both axes, thus maintaining the $\frac{A}{D}$ ratio, the shape of the rectangle and the bone storage profile. The scaling factor g is defined by equating the initial and final BMC's, hence $D \times A = (gD_0) \times (gA_0)$ and $g = \sqrt{\frac{DA}{D_0A_0}}$, thus $g = \sqrt{\frac{C}{C_0}}$. Secondly, we consider the shape transformation at constant BMC, during which the characteristic point of the bone structure moves along the hyperbola $D \times A = C$. We decompose this transformation into a transformation at constant bone

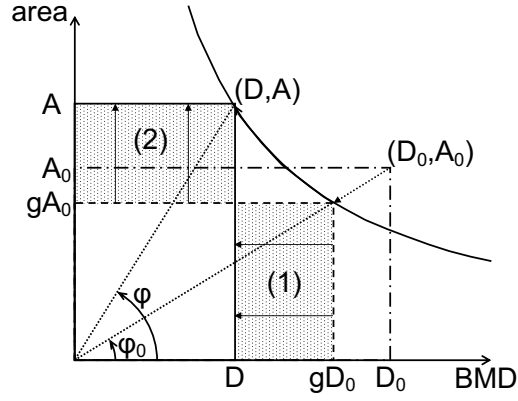

Figure 2: The density-area plane. A_0 and D_0 are the projected bone area and BMD at operation and A and D at time of follow-up. The bone storage profile is characterized by the shape of the rectangle and hence by the angle φ. Structural changes at constant content move along hyperboles of equation $D \times A = C$. Content changes at constant structures appear as scaling of the bone mineral content rectangle along its diagonal.

volume (implying constant A) followed by a transformation at constant bone density. Figure 2 illustrates a case of decreasing density and increasing volume. In the opposite case, the expressions below still apply though the quantities are negative.

1. The characteristic point of the bone structure moves from (gD_0, gA_0) to (D, gA_0). The BMC lost is $(gD_0 - D) \times gA_0$ (Figure 2, grey area 1)

2. The characteristic point of the bone structure moves from (D, gA_0) to (D, A). The BMC gained is $D \times (A - gA_0)$ (Figure 2, grey area 2).

As the combination of these two transformations preserves the BMC, we have that $(gD_0 - D) \times gA_0 = D \times (A - gA_0)$. Each of the grey areas represent the bone mass lost in density storage and gained in volume storage. The fraction of the BMC thus changing storage form is defined as the *index of structural remodelling* and reads:

$$\alpha = \frac{(gD_0 - D) \times gA_0}{C} = \frac{g^2 D_0 A_0 - gDA_0}{g^2 D_0 A_0} = 1 - \sqrt{\frac{A_0 D}{A D_0}}$$

This last expression also indicates the link to φ and φ_0:

$$\frac{\tan\varphi_0}{\tan\varphi} = (\alpha - 1)^2$$

The index of structural remodelling measures the relative amount of internal remodelling and external modelling. Thus, α and $\Delta\varphi$ are equal to zero if internal remodelling and external modelling are equal, that is D and A vary in the same proportions. Similarly, α and $\Delta\varphi$ are positive when the bone volume increases and the bone density decreases and α and $\Delta\varphi$ are negative when the bone volume decreases and the bone density increases.

2.4 Statistical analysis.

For the correlation analysis, pre-examination of the DEXA measurements showed that the samples were non-Gaussian, therefore, to study the correlation between the BMC change and the BMC at operation, we used the Spearman correlation coefficient r_S. The significance of the correlations was assessed using the distribution of sums of squares of rank differences for small samples.

For the qualitative analysis, the significance of the sign of the angle change $\Delta\varphi$ is tested by a non-parametric sign test. To enhance the test power the BMD (respectively projected bone area) is made dimensionless by dividing it by the average BMD (respectively projected bone area) over the study patients and the initial value and at time of follow-up. The average α was calculated in each Gruen zone and the significance of its sign was tested using a non-parametric sign test.

3 Results

3.1 Quantitative analysis.

All correlation coefficients were negative indicating that the relative bone loss after five years is more important for patients with higher immediate postoperative bone mass. High BMC postoperatively was significantly correlated to high relative BMC loss after five years ($P < 0.05$) in the Gruen zone R2, R4 to R7 and globally. The slopes of the linear regressions are reported in Table 1. The projected bone area postoperatively showed a poor correlation with its relative variation, which was significant in Gruen zone R2 only. Bone mineral density postoperatively was moderately correlated with its relative variation, which was

Table 1: Slopes of the linear regressions expressing the change in BMC, projected bone area or BMD as a function of their respective immediate postoperative value. The mean values of the *index of structural remodelling* α are all significantly positive ($P < 0.01$) meaning that the structural remodelling occurs systematically as an expansion.

Slope	R1	R2	R3	R4	R5	R6	R7	All zones
BMC	-0.23	-0.64**	-0.35	-0.54*	-1.04**	-0.69**	-0.31**	-0.62*
Projected bone area	-0.38	-0.79**	-0.54	-0.26	-1.11	-0.42	-0.39	-0.57
BMD	-0.09	-0.28	-0.17	-0.72*	-0.63**	-0.54*	-0.37*	-0.47*
α (%)	9.1**	11.0**	5.1**	4.4**	10.0**	12.1**	7.3**	7.1**

*$P < 0.05$ **$P < 0.01$

significant in Gruen zones R4 to R7 and globally. The slopes of the linear regressions reported in Table 1 vary greatly from -1.04 (BMC in R5) to -0.31 (BMC in R7). These two cases are illustrated in Figure 3.

3.2 Qualitative analysis.

The average index of structural remodelling α in each Gruen zone is reported in Table 1. Its value for the femur globally is 7 %, the lowest value was registered distally in R4 (4.4 %), while the highest values were obtained mid-proximally both medially and laterally with 11 % in R2 and 12 % in R6. All α-values were tested to be significantly strictly positive ($P < 0.01$), meaning that the structural remodelling, as a combination of internal remodelling and external modelling, occurs systematically as an expansion of the bone. Furthermore, the index of structural remodelling is independent of BMC, projected bone area and BMD at operation ($r_S < 0.05$, Spearman correlation) indicating that the observed tendency to expansion occurs in patients with all types of bone stock, in amount and structure, at operation time.

4 Discussion

This study shows that bone mineral content can be a quantitative predictor of bone remodelling for younger patient with custom, uncemented femoral implants. It shows furthermore that the higher the BMC at operation, the higher the relative bone loss. Femurs 20 % below the average BMC will experience an 8 % bone gain while femurs 20 % above the average BMC will experience a 10 % bone loss. The lack of correlation for the projected bone area and the

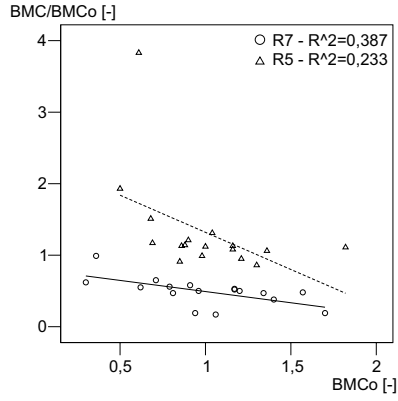

Figure 3: Relative change in bone mineral content (BMC) as a function of the dimensionless BMC at operation plotted for Gruen zones R5 and R7. The negative slopes indicate that bones with high BMC at operation have a higher relative bone loss.

weaker correlation obtained with the BMD may be attributed to the different ways of distributing the BMC between volume increase and density increase as investigated in the qualitative analysis. The latter shows that typical DEXA output variables like BMC, projected bone area and BMD can describe significantly the qualitative changes in the bone structure, which, to our knowledge has not been previously reported. Five years after implantation of a custom implant in younger patients, a significant expansion of the periprosthetic bone is observed locally and globally. The index of structural remodelling α is a relative quantity comparing the amount of internal bone remodelling and external modelling. Even if α is significantly positive, meaning a relative expansion of the bone, volume loss can occur but will probably be associated with an even higher density loss.

A previous study (Sychterz and Engh, 1996) concludes to a positive correlation between preoperative bone mineral content and its relative change. However, the population as well as the method that was used differs from the one used in the present paper. Our population sample is slightly larger (17 against 11) and the implants inserted in our study were customized prostheses as opposed to standard, straight-stem prostheses. Nevertheless, one of the

biggest discrepancies can probably be attributed to the average patient age of 48.5 years at follow-up in this analysis against 73.9 years in the study by Sychterz and Engh. This is in accordance with the difference in remodelling activity between younger and older patients, as reported by Groessner-Schreiber (1992) and Brockstedt (1991). In addition to this, the data of Sychterz and Engh (1996) were retrieved post mortem and the reference was the contralateral bone. This last difference may play a considerable role in so far as the contralateral bone has aged with the patient and therefore does not necessarily reflect the bone content preoperatively (Hall et al., 1991). In addition to this it may have remodelled before the hip replacement due to gait disability compensation. Another study (Rahmy et al., 2004) investigated the correlation of immediate postoperative bone mineral density with its relative change after three years. BMD, as opposed to BMC, does not account for external modelling though the latter can play an important role as described in this article. For example, a massive loss in bone volume can be overlooked or underestimated if the density of the remaining bone is in a normal range. Furthermore, the measure of bone remodelling used by Rahmy accounts for the whole course of the follow-up (area under the curve). This quantity, integrated over time, is difficult to compare to long-term quantities if the remodelling profiles in time are very different. For example, the pronounced bone loss three to six months after operation will have a considerable influence in the area under the curve, which is purposely disregarded for long-term considerations in the present study. Finally the average patient age of 63 was considerably older than the present study's patients. However a study on the proximal tibia after total knee arthroplasty (Li and Nilsson, 2000) shows that the postoperative BMD had a significant negative correlation with the relative changes of BMD between operation and 24 months, which supports this study's results. They observed further a correlation between postoperative BMD and the magnitude of deformity of the knee before operation thus suggesting a normalization of the BMD following the deformity correction.

The DEXA scanning we used in the present study did not allow for measurements in the sagittal plane. Data available only in frontal projection may conceal valuable information especially regarding the volume vs. density distribution of a given bone mineral content.

This work describes a method to quantify and predict the structural bone remodelling in the proximal femur after insertion of uncemented, custom femoral stems and also to identify patients at risk for increased bone loss following total hip replacement. Furthermore, structural changes in bone are of interest in

computer simulation of bone remodelling to highlight how a given mechanical signal stimulates internal remodelling or external modelling.

Acknowledgment

Professor Gunnar Leivseth MD, PhD, Department of Neuroscience, Faculty of Medicine, Norwegian University of Science and Technology, gave valuable comments on this article.

References

Brockstedt, H., Kassem, M., Eriksen, E.F., Mosekilde, L., Melsen, F., 1991. Age- and sex-related changes in iliac cortical bone mass and remodeling. *Bone* 30, 681-691.

Clohisy, J.C., Harris, W.H., 1999. The Harris-Galante uncemented femoral component in primary total hip replacement at 10 years. *J Arthroplasty* 14, 915-917.

Cohen, B., Rushton, N., 1995. Accuracy of DEXA measurement of bone mineral density after total hip arthroplasty. *J Bone Joint Surg Br* 77, 479-483.

Dorr, L.D., Lewonowski, K., Lucero, M., Harris, M., Wan, Z., 1997. Failure mechanisms of anatomic porous replacement I cementless total hip replacement. *Clin Orthop* 334, 157-167.

Eingartner, C., Volkmannm, R., Winter, E., Maurer, F., Sauer, G., Weller, S., Weise, K., 2000. Results of an uncemented straight femoral shaft prosthesis after 9 years of follow-up. *J Arthroplasty* 15, 440-447.

Engh, C.A., McGovern, T.F., Bobyn, J.D., Harris, W.H., 1992. A quantitative evaluation of periprosthetic bone-remodeling after cementless total hip arthroplasty. *J Bone Joint Surg Am* 74, 1009-1020.

Georges, A., Barthe, N., Castaing, F., Basse-Cathalinat, B., Bordenave, L., 2002. Evaluation biologique et densitometrique du remodelage osseux induit par l'arthroplastie totale de hanche. *Ann Biol Clin (Paris)* 24, 683-688.

Groessner-Schreiber, B., Krukowski, M., Lyons, C., Osdoby, P., 1992. Osteoclast recruitment in response to human bone matrix is age related. *Mech Ageing Dev* 62, 143-154.

Hall, M.L., Heavens, J., Ell, P.J., 1991. Variation between femurs as measured by dual energy X-ray absorptiometry (DEXA). *Eur J Nucl Med* 18, 38-40.

Keisu, K.S., Mathiesen, E.B., Lindgren, J.U., 2001. The uncemented fully textured Lord hip prosthesis: a 10- to 15-year followup study. *Clin Orthop* 382, 133-142.

Kilgus, D.J., Shimaoka, E.E., Tipton, J.S., Eberle, R.W., 1993. Dual-energy X-ray absorptiometry measurement of bone mineral density around porous-coated cementless femoral implants. Methods and preliminary results. *J Bone Joint Surg Br* 75, 279-287.

Kröger, H., Miettinen, H., Arnala, I., Koski, E., Rushton, N., Suomalainen, O., 1996. Evaluation of periprosthetic bone using dual-energy x-ray absorptiometry: precision of the method and effect of operation on bone mineral density. *J Bone Miner Res* 11, 1526-1530.

Larnach, T.A., Boyd, S.J., Smart, R.C., Butler, S.P., Rohl, P.G., Diamond, T.H., 1992. Reproducibility of lateral spine scans using dual energy X-ray absorptiometry. *Calcif Tissue Int* 51, 255-258.

Li, M.G., Nilsson, K.G., 2000. Changes in bone mineral density at the proximal tibia after total knee arthroplasty: a 2-year follow-up of 28 knees using dual energy X-ray absorptiometry. *J Orthop Res* 18, 40-47.

Massari, L., Bagni, B., Biscione, R., Traina, G.C., 1995. Periprosthetic bone density in uncemented femoral hip implants with proximal hydroxylapatite coating. *Bull Hosp Jt Dis* 77, 206-210.

Mortimer, E.S., Rosenthall, L., Paterson, I., Bobyn, J.D., 1996. Effect of rotation on periprosthetic bone mineral measurements in a hip phantom. *Clin Orthop* 324, 269-274.

Rahmy, A.I., Gosens, T., Blake, G.M., Tonino, A., Fogelman, I., 2004. Periprosthetic bone remodelling of two types of uncemented femoral implant with proximal hydroxyapatite coating: a 3-year follow-up study addressing the influence of prosthesis design and preoperative bone density on periprosthetic bone loss. *Osteoporos Int* 15, 281-289.

Sychterz, C.J., Engh, C.A., 1996. The influence of clinical factors on periprosthetic bone remodeling. *Clin Orthop* 322, 285-292.

Comparison of patient-specific bone remodelling simulation and five-year *in vivo* DEXA measurements

Sébastien Muller[a,b], Sune H. Pettersen[a,b], Nico Verdonschot[c] and Marco Barink[c]

[a] Faculty of Engineering Science and Technology, Department of Structural Engineering, Norwegian University of Science and Technology, Trondheim, Norway

[b] Norwegian Orthopaedic Implant Research Unit, St Olavs Hospital, MTFS, Olav Kyrresgate 3, 7489 Trondheim, Norway

[c] Orthopaedic Research Lab, Nijmegen, The Netherlands

Abstract

Younger patients with uncemented custom femoral implants often experience bone growth, which has previously been difficult to simulate correctly. This study evaluates the agreement between clinical observations and patient-specific finite element simulations. The relevance of a new memory effect is also assessed.

We modelled the thighbones and implants of 14 patients of median age 45 years at operation. The stair-climbing load case was scaled according to the patient weight. Cortical and cancellous bone was modelled as inhomogeneous anisotropic linear elastic. The mechanical stimulus for bone remodelling was the difference between the current strain energy density and the preoperative one, either modified by a memory effect for a series of simulations or unchanged for control. During the remodelling, the model is projected frontally to simulate a DEXA: bone mineral content, bone mineral density and projected bone area are calculated for each Gruen zone.

The simulated values at seven points in time and in the seven Gruen zones were compared to the corresponding clinical measurements. A non-linear model, based on the simulated relative changes of mineral content, mineral density or projected area, predicted the corresponding DEXA output very satisfyingly (all $R^2 > 0.86$, $N = 606$). The memory effect,

hypothesising that bone "forgets" its initial mechanical state, stabilized the remodelling, gave results correlating better with the clinical results, and avoided extreme, non-physiological growth.

Bone remodelling simulation in younger patients with uncemented custom femoral implants provides results in good agreement with the clinical measurements though improvement is still necessary regarding the material law.

To be submitted to *Journal of Biomechanics*.

1 Introduction

Simulation of bone remodelling has been a tool of increasing interest for the last two decades. It allows to test remodelling mechanisms and provides information that may not be measurable experimentally (Krumme et al., 1984). The first endeavours in the 1980's present models of theoretical interest (Hart et al., 1984) in non-pathological cases. More recent works study remodelling as the natural bone turnover in aging (Kubik et al., 2002) or normal healthy subjects (Langton et al., 1998; Taylor and Lee, 2003).

However, a larger part of the literature is dedicated to periprosthetic bone remodelling. It became clear that bone resorption was related to the rigidity and bonding properties of the implant (Huiskes et al., 1987; Weinans et al., 1992). Van Rietbergen et al. (1993) showed that bone remodelling simulation predicted similar amounts of proximal bone loss and distal bone densification as found in animal experiments. In another study, it was found that relative loss of bone mineral content simulated with patient-specific models corresponded very well with DEXA measurements of the corresponding retrieval bones (Kerner et al., 1999). This adaptive model based on strain energy density (SED) compares to damage-adaptive models (McNamara et al., 1997), which also reproduce some well-known clinical features (Doblaré and García, 2001). An adaptive model, based on tensile principal stress, is found to give the closest predictions to turkey ulna experimental results under the imposed conditions (Taylor et al., 2003).

However the comparison of simulated and clinical data is only qualitative (Kerner et al., 1999; Taylor et al., 2003). A comprehensive work has been done by Van Rietbergen (1993) who compared quantitatively the simulations for a specific dog to the clinical results of a group of dogs but no global estimation of the agreement was given.

The simulations by Kerner et al. (1999) overestimated bone loss and further analysis suggested that the adaptive process was limited to a finite postoperative period. They hypothesised that bone does not "remember" its preoperative state of strain after a certain time and terminates the adaptive process even though the original state is not re-established.

Extensive studies comparing quantitatively the simulation of periprosthetic bone remodelling with clinical results, based on patient-specific human models are still lacking to assess the quality of adaptive models and to compare them. In this article, we asked whether a patient-specific SED-adaptive model can predict quantitatively internal remodelling and external modelling. Additionally, we implemented a fading memory effect hypothesising that bone does not "remember" its original preoperative state after a certain time.

2 Methods

2.1 Patients.

Thirteen patients (14 hips), six women and seven men, with a median age of 45 years at operation (ranging from 20 to 59 years) and with a median weight of 76 kg (ranging from 53 to 112) underwent primary hip replacement between June 1997 and May 1998. All patients were operated by two experienced orthopaedic surgeons and received a custom uncemented femoral implant (Unique, Scandinavian Customized Prostheses, Norway). Their bone mineral content (BMC), bone mineral density (BMD) and projected bone area were monitored by dual energy x-ray absorptiometry (DEXA) for a median follow-up time of 60 months (ranging from 24 to 60 months) covered by seven controls at 0, 3, 6, 12, 24, 36 and 60 months after operation. The Merler d'Aubigné scores for gait function, mobility and pain were recorded preoperatively and at each DEXA control.

2.2 Geometrical model and mesh.

A three-dimensional model of the femur of each patient was reconstructed (Solidworks 2003, Solidworks Corporation) using contours extracted from preoperative CT-scans of 5 mm thickness and 5 mm spacing (edge to edge). Difficult features of the proximal femur (*fossa piriformes*) were handled manually following common rules for all patients. Cortical bone was modelled as an intact (preoperative) version and a resected (postoperative) one. It then was assembled with cancellous bone alone or cancellous bone and the patient's implant to form a full intact or implanted model. Each of these was meshed using Cosmos/Works 2003 (Structural Research and Analysis Corp.) with 4 mm four-noded tetrahedrons, on average 25000 elements per model.

2.3 Material properties, forces and boundary conditions.

Cortical bone was modelled as linear elastic and transverse isotropic. The mechanical properties were calculated from local apparent densities (ρ in g/cm^3) based on an anisotropic adaptation of the cubic law by Carter and Hayes (1977):

$$E = 3790\rho^3 \tag{1}$$

where E is a modulus of elasticity in MPa. A ratio of transverse to longitudinal modulus of elasticity of 0.64 was retained according to established studies on

Table 1: Mechanical properties of bone as a function of the apparent density.

	E_l or E	E_t	ν_{lt} or ν	ν_{tt}
Cortical bone	$3790\rho^3$	$2407\rho^3$	0.23	0.4
Cancellous bone	$3790\rho^3$		0.1	

bone mechanical properties (Couteau et al., 1998; Taylor et al., 2002). A maximum bone apparent density of 1.73 g/cm^3 (Weinans et al., 1993) corresponds, according to (1), to 22 GPa, which is also a common maximum value of the longitudinal modulus of elasticity. The isotropic modulus from (1) was chosen as a longitudinal modulus and scaled down to obtain the transverse modulus. Cancellous bone was modelled as linear elastic and isotropic directly using (1). Other mechanical properties are summarized in Table 1. Blurring of CTs due to finite slice width leads to underestimation of the densities in the tapered proximal region. Therefore, the immediate postoperative properties of cortical bone in the whole femur were modelled as homogeneous, adjusted for each femur on the average cortical density estimated from the three distal-most CTs where the CT blurring is negligible. During the remodelling, the material properties were applied elementwise base on a conversion of densities according to equation (1). The stair climbing loading case was applied to the model using a compressive force of 1800 N on the femoral head, a tensile force of 1200 N on the greater trochanter and an axial torque of 10 Nm as a baseline for a body weight of 70 kg. For each patient the forces were scaled proportionally according to his weight. To simulate the changing boundary conditions between implant and bone over time, a special bonding algorithm was designed. Starting with a totally de-bonded implant, the static analysis at each increment determined if sliding would occur at each point. If no local sliding greater than 20 μm (Pilliar et al., 1986; Jasty et al., 1997) was observed for more than ten consecutive increments, the implant was bonded to the bone at this node, thus imitating osseointegration. This model is similar to the scheme used by Fernandes et al. (2002) but their displacement condition had to be held only for one increment.

2.4 Remodelling and memory.

Strain adaptive remodelling as described by Weinans et al. (1993), is based on strain energy density (SED) and was the core of the model in this study. All FE simulations were performed by COSMOS (Structural Research and Analysis Corporation) and external computations were programmed in Matlab (The

MathWorkds, Inc.) The time step was constant at 0.1 month. A threshold under which no remodelling occurs, called dead zone, of 75 % was used (Kerner et al., 1999) combined with an absolute threshold on the change of SED of 500 N/g/m.

The fading memory effect (Kerner et al., 1999) hypothesizes that the bone does not "remember" its preoperative mechanical state after a certain time. This was modelled by an averaging of the reference signal where the SEDs computed for the postoperative increments gradually replace the preoperative reference value in an effect of dilution. We introduce the law of fading memory:

$$S_{ref}^{i+1} = \frac{S_{ref}^{i}(T - dt) + S^{i}dt}{T} = S_{ref}^{i} + \frac{dt}{T}(S^{i} - S_{ref}^{i})$$

where S^i is the SED computed for the current increment i, S_{ref} is the reference SED, T is a characteristic remodelling time, and dt is the remodelling increment. The characteristic remodelling time is fixed to five years, meaning that the contribution of the preoperative SED in the reference SED is only 37 % after five years. The remodelling course of all 14 hips was simulated with and without memory effect for comparison.

2.5 DEXA simulation.

At chosen points in time during the remodelling simulation, DEXA measurements were simulated. The coordinate system of the FE model was transformed to align the model on the patient's position during the DEXA examination. The density distribution and geometry of the FE model were read into a three dimensional table and projected to reproduce the DEXA control. The projection thus obtained was divided into the seven Gruen zones (Figure 1) where the bone mineral content and bone projected area were counted; there ratio gave the bone mineral density. As the Gruen zones are based on anatomical features, they could be defined in the simulated DEXA identically to the clinical measurements.

2.6 Statistical analysis.

The six variables BMC and projected bone area, either clinically measured, simulated with fading memory or without, are denoted as described in Table 2. The same variables at operation time $t = 0$ take an additional zero-superscript and the relative changes from time $t = 0$ to time t take an additional r-superscript. Each pair of clinically measured and simulated BMC corresponds to a triplet

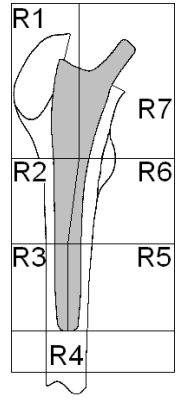

Figure 1: A right femur in frontal projection and its partition into seven Gruen zones from R1 to R7.

of the three parameters: time of DEXA control, patient, and Gruen zone. One such triplet was considered as one categorical variable. The distributions of the six variables were tested for normality (Kolmogorov-Smirnov). Simulated and clinical BMC on the one hand and projected bone area on the other hand were compared for all the occurrences of the categorical variable using Spearman correlation, linear and non-linear regression (SPSS, SPSS Inc). The Gruen zone R1 of one patient was modelled larger than the real one. The error affected six observation times, hence, from the total 637 occurrences (14 patients $\times$ seven Gruen zones $\times$ six to seven observation times), six had to be removed from the simulated results due to this design error. Ten more observations had to be removed from the clinical measurements due to erroneous definition of the Gruen zones during the clinical control, leaving $N = 606$ observations with three valid values for simulation, measurement and immediate postoperative measurement. The relative changes in BMC from the postoperative base line were compared for the clinical measurements and the BMC simulated with fading memory with a Wilcoxon signed rank test.

Table 2: Variables for statistical analysis.

	Clinical	Simulated	Simulated with fading memory
BMC	BMC_c	BMC_s	BMC_{sm}
Projected bone area	PBA_c	PBA_s	PBA_{sm}

Table 3: Correlation between clinical and simulated BMC and bone projected area.

Spearman's rho between:	Simulated	Simulated with fading memory
Clinical BMC	0.881	0.860
Clinical Projected bone area	0.875	0.856

3 Results

None of the six variables in Table 2 was normally distributed (Kolmogorov-Smirnov, $P < 0.001$). The Spearman correlation coefficients are reported in Table 3, showing significant correlations ($P < 0.01$) between the clinical and simulated values.

Simulations with memory effect fit slightly better the clinical results than those without memory effect (confirmed with Kendall correlation). Visual examination of 3D representations of the external modelling of the femur shows for some patients abnormal pattern for the simulations without memory effect. Two ridges on the latero-frontal and dorsal sides (Figure 2) appear clearly as indicated by the excess of BMC and projected bone area in Gruen zone R5 and R6. Furthermore, an excessive bone loss in R7 is observed. However, we reckon that the largest part of this erroneous effect remains in the shadow of the implant under the simulated DEXA. Based on these observations and on the better correlations achieved by the simulation with memory effect, we limit further analyses to these.

The profile of the BMC summed up over the seven Gruen zones as a function of time is reported in Figure 3. The simulated values of BMC are overestimated throughout the simulation, which is corrected for in the statistical approach. As not all patients had the 54 and 72 months controls, the values calculated at these times are not based on all patients, which explains the discontinuities. The simulations without memory effect show more bone growth after 12 to 24 months. Though this seems to correspond to the relative changes observed

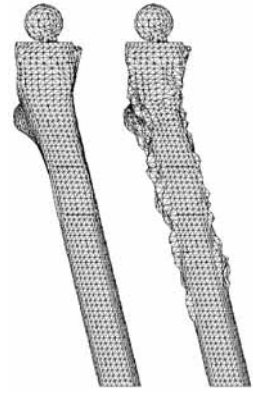

Figure 2: Meshes of a femur with implant immediately after operation and after 60 months of remodelling without memory effect. The ridges on the antero- and postero-lateral sides appear clearly as a consequence of the loading of the former neutral axis.

clinically, this compound BMC conceals an erroneous distribution of the bone growth as described above. A distribution of the BMC by Gruen zone averaged over patients and observation times shows the same overestimation by the simulations.

The relative changes in BMC from the postoperative base line were larger for the clinical measurements than for the BMC simulated with fading memory ($P < 0.05$, Wilcoxon signed rank test). This means that the simulation underestimates the relative bone growth (overestimates the relative bone loss). This difference is even more significant for the simulated values without memory effect ($P < 0.001$).

A linear regression between BMC_c and BMC_{sm} gave the following results: $\mathrm{BMC}_c = 0.554\,\mathrm{BMC}_{sm} - 0.143$, $R^2 = 0.706$, $P < 0.001$ Although this indicates that BMC_{sm} is a good predictor of BMC_c, the slope of 0.554 indicates that the simulations overestimate systematically the bone mineral content. This can be due to either a wrong estimation of the material properties based on the CTs of the patient and/ or to an erroneous remodelling model. To eliminate the latter, we proposed the following non-linear regression based on relative variation of simulated BMC from postoperative baseline: $\mathrm{BMC}_c = \mathrm{BMC}_c^0 \times (a\,\mathrm{BMC}_{sm}^r + b)$.

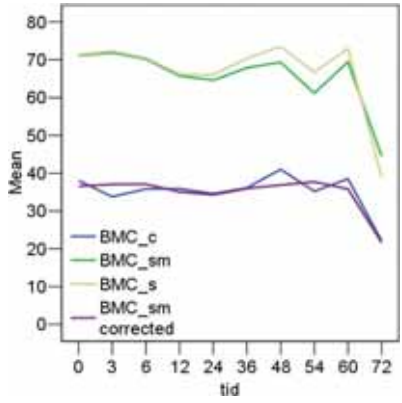

Figure 3: The total BMC in grams summed up over the seven Gruen zones as a function of time. The fluctuations, especially at 54 and 72 months, only reflect the fact that this value is based only on part of the patients as not all of them had the corresponding DEXA control.

This model, though more complex, is still relevant in a predictive perspective as it only uses simulated quantities and immediate postoperative clinical data. The regressions for bone mineral content, projected bone area (PBA) and bone mineral density gave:

$$\begin{aligned} \mathrm{BMC}_c &= \mathrm{BMC}_c^0 \times (0.613\,\mathrm{BMC}_{sm}^r + 0.348), \quad R^2 = 0.873, \\ \mathrm{PBA}_c &= \mathrm{PBA}_c^0 \times (0.698\,\mathrm{PBA}_{sm}^r + 0.371), \quad R^2 = 0.932, \\ \mathrm{BMD}_c &= \mathrm{BMD}_c^0 \times (0.582\,\mathrm{BMD}_{sm}^r + 0.328), \quad R^2 = 0.868. \end{aligned}$$

All three regressions were based on $N = 606$ observations and achieved a significance of $P < 0.001$. This model reveals BMC_c^0 and BMC_{sm}^r as very strong predictors of BMC_c and similarly for the projected bone area and BMD. The corrected values of the BMC simulated with fading memory are reported in Figure 3 as a function of time. The simulations fail to predict the immediate post-operative bone loss, which is usually believed to be traumatic and not mechanically induced. In Figure 4, the greatest mismatches between clinical BMC and corrected simulated BMC are a minor underestimation in Gruen zone R1 and an small overestimation in R7.

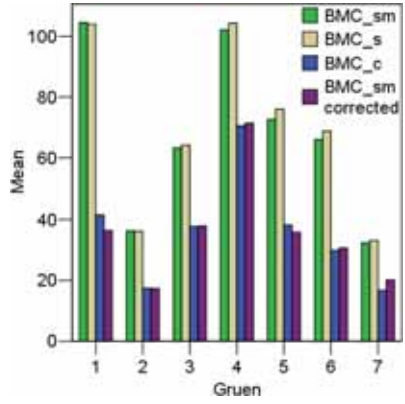

Figure 4: The BMC in grams by Gruen zone is average over patients and observation times.

4 Discussion

This study showed that patient-specific SED-adaptive FE bone remodelling models are very strong predictors of clinically observed bone remodelling. However the direct comparison of simulated BMC, projected bone area and BMD with their clinical equivalent shows that the FE simulations are interesting as predictions of relative changes rather than absolute quantities.

One can look at the results of the simulations as a contribution from the initial distribution of bone mass and a contribution from the remodelling process itself. As the non-linear regression models are based on relative changes, the better results they achieve indicate that an important component of the bias lies in the distribution of the material properties. The same need of calibration of the initial model is also reported in the work by Kerner et al. (1999). The two contributions are not totally independent though as the amount of remodelling has been shown to be dependent on initial bone stock (Sychterz and Engh, 1996). This may in turn explain the slopes and intercepts found instead of the one-to-one relationship expected between the simulated and clinical relative change of BMC, projected bone area and BMD.

The patients' score for gait function, mobility and pain were considerably improved after operation, which suggests an increased activity level and increased

loads on the femora. However, the remodelling simulation was run with identical loads pre- and postoperatively. This might explain the underestimation of the relative BMC increase observed for the simulations.

The source of error for the conversion of CT to material properties is compound. Slice thickness of the CT in proximal regions with tapered geometry causes underestimation of densities (Hangartner and Shah, 2003). This leads to an erroneous modelling of the mechanical conditions at operation with a relative weakening of the Gruen zone R7. The initial value for cortical bone was therefore based on distal slices where the blurring disappears because of the thickness of the cortical wall and the straightness of the shaft. Though this distribution represents another approximation, it appeared to be closer to the physiological distribution of bone mass.

The memory effect is suggested by Kerner et al. (1999) to account for the fact that the bone does not re-establish fully the original state, which is supposed to be forgotten. This relies implicitly on some physical storage of the original state strain in the bone tissue. Therefore, based on estimations of bone turnover (Huiskes et al., 2000) we assumed a form for the law of fading memory equivalent to an exponentially decreasing contribution of the reference SED. The characteristic time of this attenuation is chosen to be five years.

Some patients had a wrong anteversion angle of the femoral neck (leading to inward or outward feet). This was corrected by the operation as the implants were customised. This led to a distinct change of the loading pattern. The pre-operative neutral axis experienced strains representing a several hundreds of percents in relative increase. Therefore heavy bone growth was observed along the former neutral axis (Taylor et al., 2003). This is strongly stabilized by the updating of the reference signal using the fading memory. However this erroneous growth would probably be reduced if a compound load case was used instead of a single load case as in the present study.

References

Carter, D.R., Hayes, W.C., 1977. The compressive behavior of bone as a two-phase porous structure. *J Bone Joint Surg Am* 59, 954-962.

Couteau, B., Hobatho, M.C., Darmana, R., Brignola, J.C., Arlaud, J.Y., 1998. Finite element modelling of the vibrational behaviour of the human femur using CT-based individualized geometrical and material properties. *J Biomech* 31, 383-386.

Doblaré, M., García, J.M., 2001. Application of an anisotropic bone-remodelling model based on a damage-repair theory to the analysis of the proximal femur before and after total hip replacement. *J Biomech* 34, 1157-1170.

Fernandes, P.R., Folgado, J., Jacobs, C., Pellegrini, V., 2002. A contact model with ingrowth control for bone remodelling around cementless stems. *J Biomech* 35, 167-176.

Hangartner, T.N., Shah, D., , 2003. Modeling of blurring due to finite slice width in computed tomography. In *Proceedings of the World Congress on Medical Physics and Biomedical Engineering [CD-ROM]*. Anonymous. pp Paper No 1652. , Sydney, Australia.

Hart, R.T., Davy, D.T., Heiple, K.G., 1984. A computational method for stress analysis of adaptive elastic materials with a view toward applications in strain-induced bone remodeling. *J Biomech Eng* 106, 342-350.

Huiskes, R., Ruimerman, R., van Lenthe, G.H., Janssen, J.D., 2000. Effects of mechanical forces on maintenance and adaptation of form in trabecular bone. *Nature* 405, 704-706.

Huiskes, R., Weinans, H., Grootenboer, H.J., Dalstra, M., Fudala, B., Slooff, T.J., 1987. Adaptive bone-remodeling theory applied to prosthetic-design analysis. *J Biomech* 20, 1135-1150.

Jasty, M., Bragdon, C., Burke, D., O'Connor, D., Lowenstein, J., Harris, W.H., 1997. In vivo skeletal responses to porous-surfaced implants subjected to small induced motions. *J Bone Joint Surg Am* 79, 707-714.

Kerner, J., Huiskes, R., van Lenthe, G.H., Weinans, H., van Rietbergen, B., Engh, C.A., Amis, A.A., 1999. Correlation between pre-operative periprosthetic bone density and post-operative bone loss in THA can be explained by strain-adaptive remodelling. *J Biomech* 32, 695-703.

Krumme, H., Guenay, M., Nagel, H.H., Delling, G., 1984. Computerized simulation of bone remodeling: graphic demonstration of dynamic processes. *Metab Bone Dis Relat Res* 5, 253-257.

Kubik, T., Pasowicz, M., Tabor, Z., Rokita, E., 2002. Optimizing the assessment of age-related changes in trabecular bone. *Phys Med Biol* 47, 1543-1553.

Langton, C.M., Haire, T.J., Ganney, P.S., Dobson, C.A., Fagan, M.J., 1998. Dynamic stochastic simulation of cancellous bone resorption. *Bone* 22, 375-380.

McNamara, B.P., Taylor, D., Prendergast, P.J., 1997. Computer prediction of adaptive bone remodelling around noncemented femoral prostheses: the relationship between damage-based and strain-based algorithms. *Med Eng Phys* 19, 454-463.

Pilliar, R.M., Lee, J.M., Maniatopoulos, C., 1986. Observations on the effect of movement on bone ingrowth into porous-surfaced implants. *Clin Orthop* 208, 108-113.

Sychterz, C.J., Engh, C.A., 1996. The influence of clinical factors on periprosthetic bone remodeling. *Clin Orthop* 322, 285-292.

Taylor, D., Lee, T.C., 2003. Microdamage and mechanical behaviour: predicting failure and remodelling in compact bone. *J Anat* 203, 203-211.

Taylor, W.R., Roland, E., Ploeg, H., Hertig, D., Klabunde, R., Warner, M.D., Hobatho, M.C., Rakotomanana, L., Clift, S.E., 2002. Determination of orthotropic bone elastic constants using FEA and modal analysis. *J Biomech* 35, 767-773.

Taylor, W.R., Warner, M.D., Clift, S.E., 2003. Finite element prediction of endosteal and periosteal bone remodelling in the turkey ulna: effect of remodelling signal and dead-zone definition. *Proc Inst Mech Eng [H]* 217, 349-356.

Van Rietbergen, B., Huiskes, R., Weinans, H., Sumner, D.R., Turner, T.M., Galante, J.O., 1993. ESB Research Award 1992. The mechanism of bone remodeling and resorption around press-fitted THA stems. *J Biomech* 26, 369-382.

Weinans, H., Huiskes, R., Grootenboer, H.J., 1992. The behavior of adaptive bone-remodeling simulation models. *J Biomech* 25, 1425-1441.

Weinans, H., Huiskes, R., van Rietbergen, B., Sumner, D.R., Turner, T.M., Galante, J.O., 1993. Adaptive bone remodeling around bonded noncemented total hip arthroplasty: a comparison between animal experiments and computer simulation. *J Orthop Res* 11, 500-513.

Viscoelastic modelling of impacted morsellised bone accurately describes unloading behaviour:

an experimental study of stiffness moduli and recoil properties

Lars Fosse[a,c], Sébastien Muller[a,b], Helge Rønningen[c], Fridtjov Irgens[b] and Pål Benum[a,c]

[a] Norwegian Orthopaedic Implant Research Unit, St Olavs Hospital, MTFS, Olav Kyrresgate 3, 7489 Trondheim, Norway

[b] Faculty of Engineering Science and Technology, Department of Structural Engineering, Norwegian University of Science and Technology, Trondheim, Norway

[c] Department of Neuroscience, Faculty of medicine, Norwegian University of Science and Technology, Trondheim, Norway.

Abstract

Morsellised bone impaction grafting is commonly used for revision arthroplasty surgery. Several reports have described the mechanical behaviour of this bone material during impaction and loading. In this study we observed the unloading progress. The loose morsellised bone was modified by particle size, particle size distribution, water and fat content. Bone pellets were constructed using different impaction energies. After impaction, the pellets were loaded statically, after which their swelling was recorded at three unloading levels. We deduced two time-dependent recoil properties, the time resistant number (TRN) and the half total swelling time (HTST), and also one stiffness property, the unloading confined modulus of elasticity (UCME). In impacted morsellised bone, the progress of swelling is visco-elastic. Bone pellets with an even distribution of particle sizes have the most rapid recoil. Those with a high liquid content recoil more slowly, and to a significantly greater extent, than pellets with low liquid content. The recoil of pellets with low liquid content is instantaneous, i.e. unrecordable, and the displacement is significantly less than in other pellet samples.

Submitted to *Journal of Biomechanics*.

1 Introduction

The impaction of morsellised bone grafts, as recommended by Sloof (1996) and Ling (Gie et al., 1993), has significantly improved survival in revision hip joint surgery (Edwards et al., 2003; Halliday et al., 2003; Schreurs et al., 2003). Several experimental studies describe how impaction force, particle size and particle mass moisture can influence the mechanical behaviour of impacted morsellised bone during impaction and load (Brewster et al., 1999; Dunlop et al., 2003; Fosse et al., 2004; Voor et al., 2004).

Morsellised bone rebounds after impaction (Ullmark and Nilsson, 1999), but the clinical effect of this swelling on the initial stability of the revised prosthesis is unknown (Masterson et al., 1997). This experimental study addresses impacted morsellised bone during unloading. We have applied a viscoelastic recoil model and analysed the extent to which it can adequately describe swelling behaviour. Which factors influence the recoil of impacted bone? Are confined loading stiffness moduli correlated to the rebound behaviour of impacted morsellised bone?

2 Methods

Juxta-articular fresh bovine bone was used. Connective tissue including joint cartilage was removed and deep frozen (-26°C) until use. Thus water and fat content were considered undisturbed. It was thawed and morsellised in a Howex 100 bone-grinding mill (HOWEX AB, Gävle, Sweden), and then kept deep frozen (-26°C) for later impaction into pellets. We varied particle distribution and particle size, water and fat content, and impaction energy. The pellets were then tested for stiffness during loading and swelling behaviour during unloading.

2.1 Varying particle distribution and particle size

The bone mill produces morsellised bone from three different cutting drums (Drum I – III). The loose bone chips produced by each drum are sieved (Analysensieb DIN ISO 3310, Fritsch, Laborgertebau, Idar-Oberstein, Germany) and described according to their particle distribution and particle size. Native bone from each drum and five sieved portions of controlled particle sizes were impacted into pellets by the standard procedure (described later), Table 1.

Table 1: Overview over the conditions in which the different studies were carried out. The cells are filled explicitly only when the conditions differ from the standard study otherwise with a hyphen. For the diameter column (d_s), the cells are filled only when the bone particles have been sieved.

Study	Study number	N	Drop height [mm]	No. of strokes	Bone mill drum	d_s[mm]	Water content	Fat content
Standard	**1**	**7**	**200**	**10**	**I**		**native**	**native**
Particle size distribution & particle size	7	6	-	-	II		-	-
	8	5	100	-	II		-	-
	11	7	-	-	III		-	-
	12	3	-	-	sieved	$d_s < 2$	-	-
	13	5	-	-	sieved	$2 < d_s < 3$	-	-
	14	8	-	-	sieved	$3 < d_s < 4$	-	-
	15	4	-	-	sieved	$4 < d_s < 5$	-	-
	16	5	-	-	sieved	$d_s > 5$	-	-
Liquid content	9	5	-	-	-		low	high
	10	14	-	-	-		low	low
	17	6	-	-	-		low	-
	18	6	-	-	-		high	-
Energy	2	7	100	-	-		-	-
	3	7	400	-	-		-	-
	4	7	400	5	-		-	-
	5	7	-	5	-		-	-
	6	7	100	5	-		-	-

2.2 Varying the water and fat content

The water and fat content of four portions of the native bone were modified (Fosse et al., submitted). The portions were impacted into bone pellets by our standard impaction procedure.

2.3 Construction of bone pellets for testing under confined conditions

Our tests were performed on impacted morsellised bone. To make the first layer of one bone pellet, three grams of loose bone granulate were fed into the impaction chamber (10.0 $cm^2 \times 1.5$ cm), and then impacted by a slap hammer (660 grams) as described below. This filling procedure was repeated until the bone chamber was full. A filled impaction chamber was called a bone pellet (Fosse et al., 2004).

2.4 Varying impaction energy

Six impaction energy levels were compared: drop heights 100, 200 or 400 mm and five or ten blows of the slap hammer per layer, Table 1. The standard impaction procedure consisted of ten impactions with a drop height of 200 mm on each layer of loose native bone. Native loose bone produced in bone mill drum I was used for all six samples (Fosse et al., 2004).

2.5 Measurements

After construction, the pellets were described by their apparent mass density (AMD). They were loaded (load head speed 10 mm/min, seven steps, each held for 20 minutes) in a load machine (Lloyd instruments, LR 10K with load cell DCL 2.5 kN) to obtain the load deformation characteristic. During impaction and loading, different stiffnesses were measured for correlation to unloading behaviour (Fosse et al., 2004). After the load test, a subsequent three-level unloading was performed on all pellets. The steps were 2300 N to 200 N, 200 N to 45 N and 45 N to 10 N. Load head speed was 10 mm/min. Recoil was assessed as the pellet height increase at each load level (200 N, 45 N and 10 N). The levels were held for 20 minutes. The axial displacements of the top of the pellets were registered as a function of time.

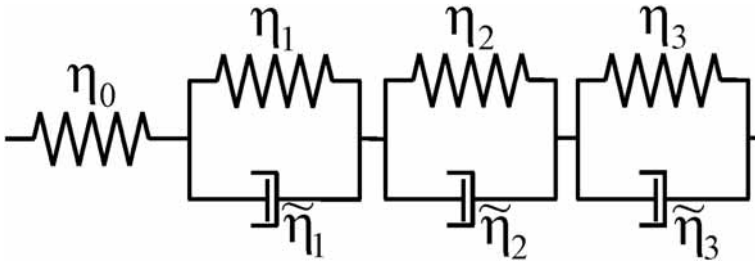

Figure 1: The generalised Kelvin model consisting of one spring and three Kelvin elements (spring and damper in parallel).

2.6 Processing experimental data

The unloading displacement data were transformed to natural strains $\varepsilon(t)$, suitable for large deformations:

$$\varepsilon(t) = \ln\left(\frac{h_0 - d(t)}{h_0}\right)$$

where h_0 is the initial height of the pellet, and $d(t)$ is the displacement of the top of the sample at time t. The regression equation to fit the observations was a generalised Kelvin model that agrees with most linear viscoelastic behaviours, having three Kelvin elements in a combination of springs and dampers, Figure 1. The relationship between strain ε and time t, is given by:

$$\frac{\varepsilon(t)}{\sigma^*} = \frac{1}{\eta_0} + \sum_{i=1}^{3} \frac{1}{\eta_i}\left(1 - \exp\left(-\frac{t}{\tau_i}\right)\right) \tag{1}$$

where η_i is the compliance of the ith spring, $\tau_i = \tilde{\eta}_i/\eta_i$ is the characteristic relaxation time of the ith Kelvin element, and σ^* the effective stress for the current unloading level (see Appendix). The seven parameters were computed by fitting the experimental data using an iterated least square method. As the interpolation for all samples was very good ($R^2 > 0.95$), the interpolating function $\varepsilon(t)$ is used in further calculations instead of the observations.

At early stages of the data analysis, some samples appeared to have an approximately constant state of strain. Though the Kelvin model is able to

approximate a constant strain, its adjustment to measurement noise could lead to meaningless and unusable regressions. We therefore handled those samples separately, based on the spread of the strain around its average. If the coefficient of variation (CV) exceeded 2 %, the regression with a Kelvin model was computed, otherwise, the strain was declared constant.

Based on characterization methods from soil engineering, we developed a parameter describing the behaviour of morsellised bone under swelling (Janbu, 1963). We defined the *time resistance* R, as the derivative of time (in seconds) with respect to strain: $R = dt/d\varepsilon$. R is the inverse of a strain rate and expresses the time required to reach a unit strain. It can be interpreted as inertia or as the tendency not to swell as time passes. Hence a high value of R implies a low swelling speed and vice versa. Figure 2 shows a typical profile of R as a function of time. For most samples, R increased almost linearly with time. Thus the slope of the approximated straight line denoted "linear regression" provides interesting and concise information. This slope is called *time resistance number* (TRN), denoted r_S. It describes the rate at which the time resistance R increases as a function of time. In other words, a high r_S means rapidly increasing time resistance, which is reflected on strain-time curves as a quick flattening. A low time resistance number on the other hand implies a slowly increasing inertia to swelling, reflected as a slow flattening of the strain-time curve. However r_S does not indicate anything about the amplitude of the corresponding swelling. The linear regression is computed based on the first 300 seconds of unloading.

The expression of $\varepsilon(t)$ in equation (1) allows us to compute a strain after letting the sample swell indefinitely:

$$\frac{\varepsilon_\infty}{\sigma^*} = \sum_{i=0}^{3} \frac{1}{\eta_i}$$

Hence we define the *half total swelling time* (HTST), denoted $t_{1/2}$, as the time taken by the sample to reach half of its possible swelling, given as a change in strain. It is thus calculated by equating the expression of the strain from equation (1), with the middle strain between $t = 0$ and infinity:

$$\varepsilon(t_{1/2}) = \frac{\varepsilon(0) + \varepsilon_\infty}{2}$$

HTST is related to the time resistance number, and a high TRN implies a short duration of the swelling process, i.e. the sample quickly reaches half of its possible swelling. Thus a high TRN is implies a short HTST.

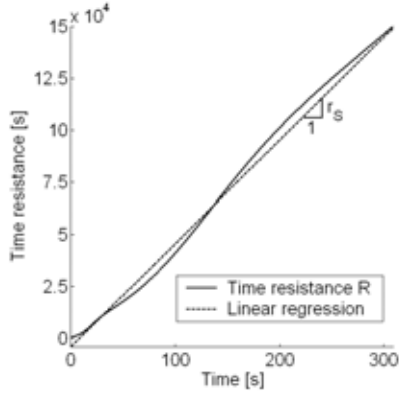

Figure 2: Time resistance R as a function of time. The approximately linear behaviour was utilized to define the time resistance number r_S.

We defined a global *unloading constrained modulus of elasticity* (UCME) for the pellet as the ratio of change in stress to change in strain from the state of maximum compression to equilibrium based on the forecast ε_∞ for the samples fitting the Kelvin model. For the remaining samples, with constant strain after unloading, the median value of the observations is used to estimate this constant state of strain.

2.7 Statistics

We used the coefficient of variation to describe how the recoil measures fitted the regression model. Statistical significance was evaluated by a two-tailed unpaired Mann-Whitney U-test. Each study outcome — time resistance number (TRN), half total swelling time (HTST), and unloading constrained modulus of elasticity (UCME) — was compared to the native sample impacted by the standard procedure, and significance was assessed by Mann-Whitney unpaired non-parametric test. The effect of each study factor was estimated using a general linear model (GLM), (Kirk, 1982), on all except for the three dry samples, totally 15 samples ($n_{total} = 88$), Table 1. Significance was assessed by multifactorial ANOVA. The influence of factor categories was established using the

percentage distribution of the parameter estimate. Loading and unloading outcome parameters were tested for correlation by Spearman rank correlation. For all analyses, $P < 0.05$ was regarded as significant. Statistical calculations were performed in SPSS (SPSS Inc, USA).

3 Results

The coefficient of variation of the pellets of low water content (groups 9, 10, and 17) was less than 2 %; their mean CV differed ($P < 0.001$) from those of groups with high water content, and they responded to unloading by an instantaneous swelling. Therefore, their time resistance number (TRN) and half total swelling time (HTST) were not defined. The TRN per sample is summarised in Table 2.

HTST values could not be computed for three bone pellets out of 276; they were removed from further calculations. Due to log failure during unloading, the HTST could not be computed for 11 pellets in studies 5 and 15. However, computation of the TRN, which is robust to missing data, was not impaired. The remaining data was is described statistically in Table 2. The unloading constrained modulus of elasticity (UCME) for each sample is summarized in Table 2. The pairwise differences for TRN, HTST, and UCME between unloading levels are significant (Wilcoxon, $P < 0.001$).

3.1 Correlation of load properties and recoil properties

During construction of the bone pellets, we measured stiffness as the impact constrained modules of elasticity (ICME). Impacted pellets were described by their apparent mass density (AMD). The load-deformation characteristic was obtained from a load machine. According to classical drainage theory, we defined the loading stiffness as the consolidated constrained modulus of elasticity (CCME) and the total constrained modulus of elasticity (TCME). There were significant positive correlations between ICME, CCME, and TCME and the time resistant number (TRN). CCME and TCME also correlated positively with the global unloading constrained modulus of elasticity (UCME). However, there was no correlation between the half total swelling time (HTST) and impaction or load properties (Table 3).

Table 2: Time resistance number (TRN), half total swelling time (HTST) and unloading constrained modulus of elasticity (UCME) for unloading step 1 for each study, given as median (median deviation). TRN and HTST are not defined (ND) for studies 9, 10 and 17 and the HTST was not calculated for studies 5 and 15.

Study	N	TRN [-]	HTST [s]	UCME [MPa]
1	7	619 (60.1)	15.2 (2.1)	24.6 (1.7)
7	6	368 (70.1)**	18.5 (2.2)	32.8 (0.2)**
8	5	327 (49.6)*	17.4 (3.4)	30.2 (1.0)*
11	7	762 (143.3)	13.1 (1.8)	24.2 (2.1)
12	3	486 (94.3)	14.5 (0.5)	21.6 (0.6)
13	5	664 (46.0)	13.7 (0.5)	44.4 (1.7)**
14	8	706 (43.5)	14.2 (1.7)	43.3 (2.8)**
15	4	636 (81.7)	-	38.8 (7.0)*
16	5	545 (35.5)	17.0 (0.7)	29.3 (0.7)
9	4	ND	ND	50.9 (3.2)**
10	11	ND	ND	47.0 (3.6)**
17	6	ND	ND	53.5 (6.6)**
18	6	326 (10.7)**	24.3 (3.6)**	28.7 (2.1)
2	7	533 (46.8)	15.3 (1.5)	43.9 (15.0)
3	7	565 (7.7)	15.6 (1.7)	29.9 (1.2)*
4	6	476 (57.1)*	17.9 (1.7)	25.3 (2.5)
5	7	364 (13.2)**	-	29.1 (2.8)
6	6	329 (27.6)**	18.3 (1.0)	29.3 (0.6)

* compared to study 1 (Mann-Whitney, $P < 0.05$)

** compared to study 1 (Mann-Whitney, $P < 0.01$)

3.2 Factorial analysis

Particle size distribution. Drum I produced mostly smaller particles of relatively uniform distribution, while Drums II and III produced morsellised bone with a greater spread of particle size. The median particle size was smallest in Drum I (2.0 mm) and largest in Drum III (3.2 mm). Bone pellets from Drum II had significantly lower time resistant numbers (TRN) than that from the other drums, while the their recoil stiffness was significantly higher than in the standard impaction study.

Particle size. There were no significant differences in TRN or half total swelling time (HTST) between pellets constructed from bone material of controlled sizes, compared to the unsieved impacted bone from Drum I. However, stiffness during recoil increased significantly, when comparing diameters of 2-3 mm, 3-4 mm, and 4-5 mm to the pellets made of unsieved bone of Drum I.

Table 3: Spearman Rank correlations between loading stiffnesses and unloading output parameters.

	TRN	HTST	UCME
AMD	0.034	0.092	0.062
ICME	0.210*	0.106	0.036
CCME	0.642**	-0.038	0.386**
TCME	0.598**	-0.074	0.335**

* $P < 0.05$ (two-tailed)

** $P < 0.01$ (two-tailed)

AMD: apparent mass density

ICME: impaction constrained modulus of elasticity

CCME: consolidated constrained modulus of elasticity

TCME: total constrained modulus of elasticity

TRN: time resistance number

HTST: half total swelling time

UCME: unloading constrained modulus of elasticity

Fat and water content. Swelling commenced almost instantaneously in bone pellets of low water content (but varying fat content). TRN and HTST were not defined. The unloading stiffness UCME, however, increased significantly by almost twice that of samples of unmodified bone constructed by the same impaction energy.

Impaction energy. The time resistant number (TRN) recorded for bone pellets impacted by 5 strokes per layer was significantly lower than that of the standard impaction (slap hammer drop height 200 mm, 10 impactions per bone layer). Increasing the drop height to 400 mm produced a significantly greater recoil stiffness — described as the unloading constrained modulus of elasticity (UCME) — than that of the standard impaction study.

Linear modelling showed that all factors (drop height, number of strokes, water content, particle size and particle size distribution) significantly affected the time resistant number (TRN). Particle size distribution was the main contributor (41 %), Table 4. Morsellised bone from Drum II, only 5 impaction strokes per layer, high water content, and particle size less than 2 mm or greater than 5 mm all significantly diminished TRN. The only sample with a significantly

increased TRN was morsellised bone from Drum III. Controlling the sizes of bone particles significantly affected both the half total swelling time (HTST) and the unloading constrained modulus of elasticity (UCME): 4-5 mm particles increased the HTST, and particles with 2-3 mm, 3-4 mm, and 4-5 mm low water content increased the UCME.

Table 4: For each of the unloading output parameters (columns), the general linear model gives the factors (rows) of significant influence, the percentage of their contribution among the significant parameter estimate (PE) and which category of the given factor contributes positively (pos.) or negatively (neg.) on the output parameter.

	TRN			HTST			UCME		
	PE (%)	Neg.	Pos.	PE (%)	Neg.	Pos.	PE (%)	Neg.	Pos.
Particle size distribution	41	drum II	drum III	-	-	-	-	-	-
Particle size	16	$d < 2$, $d > 5$	-	100	-	$4 < d < 5$	51	-	$2 < d < 5$
Fat content	-	-	-	-	-	-	-	-	-
Water content	22	high	-	-	-	-	49	-	low
Drop height	-	-	-	-	-	-	-	-	-
Number of strokes	21	5	-	-	-	-	-	-	-

4 Discussion

This study shows that the swelling behaviour of impacted morsellised bone can be accurately described by a simple linear viscoelastic material model, as witnessed by the very low values of the relative mean square errors. At the microscopic level, viscous behaviour is associated with fluid flow between the bone particles. The elastic component is associated with the deformation (bending) of long particles, or spikes on irregular particles.

In an earlier study, Ullmark and Nilsson showed that impaction force and particle size significantly influence recoil behaviour (Ullmark and Nilsson, 1999). We have shown that liquid content and bone particle size significantly influence the mechanical behaviour of impacted bone during recoil. The three samples with non-viscoelastic behaviour (9, 10 and 17) can be interpreted as having degenerated from the Kelvin model to a single spring. The instantaneous relaxation of the sample when unloaded is purely elastic. The absence of viscosity can be explained by the reduced fluid flow through the pores of the material

as the total fluid content is reduced. As for the high impaction energies, the reduced compliance under recoil (higher stiffness) for the dried samples may be explained by partial crushing of the bone particles, which thereby lose their elastic energy. We hypothesise that water, as an incompressible fluid, protected the bone particles from the blows in the other cases.

The swelling process appears to be rapid for all samples. In those slowest to swell, 50 % of the total swelling remained after 25 seconds of the first unloading step; recoil then continued more slowly. However, the pellets still had some remaining expanding tension. During joint revision surgery, the morsellised bone is impacted, and then cement is injected into the cavity formed by the impaction device (a piston with the same shape as the current prosthesis). The prosthesis is inserted during the final setting phase of the cement. Before insertion, the cement is compressed proximally to achieve global and optimal penetration into the impacted bone. Whether this applied counter pressure affects bony recoil is unknown, but it may postpone its progress. With recoil deformation left, there will still be a tension that may grip the prosthesis and the surrounding cement envelope, thus further stabilising the prosthesis. It would require further studies to investigate whether this mechanism increases the initial stability of the revised prosthetic system.

Clinical studies have focused on the thickness of the cement mantle between the new prosthesis and the impacted bone. A mantle less than 2 mm thick is at increased risk of early aseptic loosening (Masterson et al., 1997; Leopold et al., 2000). Morsellised bone impaction in the femur, with a piston shaped like the double tapered prosthesis, may deliverer different impaction energies proximally and distally in the femoral canal. The double tapered shape also increases the thickness of the impacted wall distally. Our results suggest that, if the distal thicker impaction layer is looser, the recoil will cause a relatively larger expansion, which may reduce the space available for cement filling; a thinner cement layer may thus impair the distal stability of the prosthetic system.

Clinically, the morsellised bone is dried in portions by twining it in a gauze swab. Radial grading of liquid content may occur in some portions. The overall liquid content may differ between dried portions. Impacting the bone, portion by portion, may lead to an impacted wall of bone with varying liquid content, causing inhomogeneous impaction and jeopardising stability.

5 Conclusion

Maximum stability during loading and unloading can be achieved by experimentally impacted, morsellised bone with low water content, containing particles of large mean size, and with a well-graded particle size distribution. During revision arthroplasty, these factors should be optimised to secure crucial initial stability.

References

Brewster, N.T., Gillespie, W.J., Howie, C.R., Madabhushi, S.P., Usmani, A.S., Fairbairn, D.R., 1999. Mechanical considerations in impaction bone grafting. *J Bone Joint Surg Br* 81, 118-124.

Dunlop, D.G., Brewster, N.T., Madabhushi, S.P., Usmani, A.S., Pankaj, P., Howie, C.R., 2003. Techniques to improve the shear strength of impacted bone graft: the effect of particle size and washing on the graft. *J Bone Joint Surg Am* 85-A, 639-646.

Edwards, S.A., Pandit, H.G., Grover, M.L., Clarke, H.J., 2003. Impaction bone grafting in revision hip surgery. *J Arthroplasty* 18, 852-859.

Fosse, L., Muller, S., Rønningen, H., Irgens, F., Benum, P., submitted. Viscoelastic modelling of impacted morsellised bone accurately describes unloading behaviour: an experimental study of stiffness moduli and recoil properties. *J Biomech*

Fosse, L., Rønningen, H., Lund-Larsen, J., Benum, P., Grande, L., 2004. Impacted bone stiffness measured during construction of morsellised bone samples. *J Biomech* 37, 1757-1766.

Gie, G.A., Linder, L., Ling, R.S., Simon, J.P., Slooff, T.J., Timperley, A.J., 1993. Impacted cancellous allografts and cement for revision total hip arthroplasty. *J Bone Joint Surg Br* 75, 14-21.

Halliday, B.R., English, H.W., Timperley, A.J., Gie, G.A., Ling, R.S., 2003. Femoral impaction grafting with cement in revision total hip replacement. Evolution of the technique and results. *J Bone Joint Surg Br* 85, 809-817.

Janbu, N., 1963. Soil compressibility as determined by oedometer and triaxial tests. In *Proceedings, European Conference on Soil Mechanics and Foundation Engineering*. Anonymous, Wiesbaden.

Kirk, R.E., , 1982. Introduction to the general linear model. In *Experimental design: procedures for the behavioral sciences*. Kirk, R.E.pp 173-180. Brooks/ Cole, Pacific Grove, California.

Leopold, S.S., Jacobs, J.J., Rosenberg, A.G., 2000. Cancellous allograft in revision total hip arthroplasty. A clinical review. *Clin Orthop* 371, 86-97.

Masterson, E.L., Masri, B.A., Duncan, C.P., 1997. The cement mantle in the Exceter impaction allografting technique. A cause for concern. *J Arthroplasty* 12, 759-764.

Schreurs, B.W., Thien, T.M., de Waal Malefijt, M.C., Buma, P., Veth, R.P., Slooff, T.J., 2003. Acetabular revision with impacted morselized cancellous bone graft and a cemented cup in patients with rheumatoid arthritis: three to fourteen-year follow-up. *J Bone Joint Surg Am* 85-A, 647-652.

Slooff, T.J., Buma, P., Schreurs, B.W., Schimmel, J.W., Huiskes, R., Gardeniers, J., 1996. Acetabular and femoral reconstruction with impacted graft and cement. *Clin Orthop* 324, 108-115.

Ullmark, G., Nilsson, O., 1999. Impacted corticocancellous allografts: recoil and strength. *J Arthroplasty* 14, 1019-1023.

Voor, M.J., White, J.E., Grieshaber, J.E., Malkani, A.L., Ullrich, C.R., 2004. Impacted morselized cancellous bone: mechanical effects of defatting and augmentation with fine hydroxyapatite particles. *J Biomech* 37, 1233-1239.

Appendix

A linear model implies that the strain is the superposition of a compressed state before the beginning of the unloading, and a tensile loading. This allows us to derive the creep function for each unloading level by subtracting the stress at the end of the previous level from the current stress level.

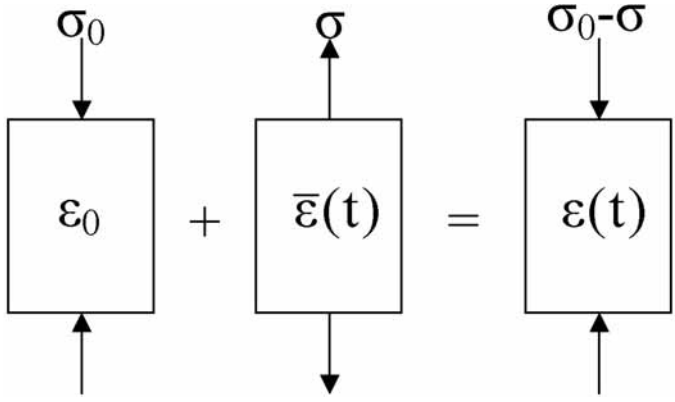

Morsellised bone under compression and torsion in femoral canal-like cavity:

comparison of finite element simulations and experimental data

Sébastien Muller[a,b], Lars Fosse[b] and Fridtjov Irgens[a]

[a] Faculty of Engineering Science and Technology, Department of Structural Engineering, Norwegian University of Science and Technology, Trondheim, Norway

[b] Norwegian Orthopaedic Implant Research Unit, St Olavs Hospital, MTFS, Olav Kyrresgate 3, 7489 Trondheim, Norway

Abstract

Morsellised bone is broadly used in revision hip surgery. However its mechanical properties are scarcely understood. They have been examined, in a previous study by Fosse et al. (Paper III, submitted), during axial unloading. The present work reports experimental results in a geometry mimicking the femoral canal under compressive and shear loading, and evaluates the continued validity of the solid linear viscoelastic model in this new configuration.

A steel cylinder with tapered cavity and fitting steel spear mimics a femoral canal and orthopaedic implant. Morsellised bone is filled into the cavity and impacted with the spear and then loaded axially with 1000 N for 120 min. Axial torsion of 6 Nm is then added and held for 120 more minutes. Axial displacement and rotation of the spear are registered as functions of time. Additionally a finite element model is designed, using Abaqus, reproducing the spear and a layer of morsellised bone surrounding it. The contact between the polished surface of the steel spear and ground bone is assumed nearly frictionless and the contact with the rough steel of the cavity is assumed fixed. The Abaqus material model is a so-called time domain viscoelasticity corresponding to a generalised Kelvin model.

The experiment showed a slowly increasing displacement of the spear sharply accelerated by the torsion. The FE model managed to reproduce qualitatively the experimental results but did not reach the very large

displacements observed. These results suggest that morsellised bone has a low cohesion and therefore behaves like a viscoplastic fluid.

In preparation for submission to *Clinical Biomechanics*.

1 Introduction

Many studies have explored the *in vivo* mechanical behaviour of bone grafts with respect to implant stability (Capello, 1994; Kärrholm et al., 1999; Pekkarinen et al., 2000). However, its mechanical properties as a material have mostly been investigated during the last five to ten years with help of geotechnical methods usually employed to study soils. The bone particles usually applied in surgery were found to have a poor grading by geotechnical standards as an optimal distribution should be very broad and include both finer and larger particle (Brewster et al., 1999). Study of the recoil properties by Ullmark et al. (1999) showed that finer particles and higher impaction force cause larger recoil. The different procedure followed by Fosse et al. (Paper III, submitted) provides quite different results thus suggesting that the grading of the particles may matter more than their average size. This viscoelastic aspect was investigated more deeply by Giesen et al. (1999) who established the existence of large irreversible deformations caused by flow-independent creep behaviour due to rolling and sliding of the bone particles. The close relationship between confined compression modulus and permeability shown by Giesen et al. (1999) suggests an influence the fluid content in morsellised bone. Voor er al. (2004) established that uniaxial compressive strain was significantly decreased in defatted bone grafts.

The stability of bone grafts between lumbar spine segments has been examined using the finite element method (Zander et al., 2002a-b) but to our knowledge, finite element analysis has not been used to validate a material model for morsellised bone. A previous study by Fosse et al. (Paper III, submitted) modelled successfully morsellised bone under compression in a cylindrical containers as a linear viscoelastic solid. We asked therefore in this article whether the same model could represent the behaviour of morsellised bone in a cavity mimicking the femoral canal under compression and torsion.

2 Methods

Connective tissue and cartilage were removed from juxta-articular fresh bovine bone that was deep-frozen at -26°C until further use. It then was thawed and morsellised in a Howex 100 bone grinding mill (Howex AB, Gävle, Sweden).

A pyramid-like cavity in a steel cylinder, illustrated in Figure 1, was filled with morsellised bone and impacted with a spear whose shape fitted exactly the cavity: ten strokes with a slap hammer weighing 660 g dropped from 200 mm.

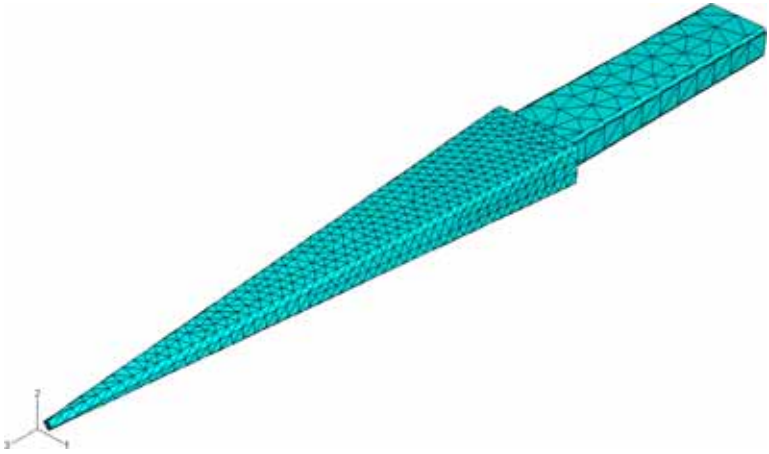

Figure 1: The mesh of the steel spear, covered with the layer of impacted morsellised bone.

More morsellised bone was fed into the cavity on the top of this first layer and the operation was repeated until the cavity was full. Then the cavity and the spear were mounted in a loading machine (Lloyd instruments, LR 10K with load cell DCL 2.5 kN). In a first step of 7200 seconds (two hours) the spear was loaded axially at 1000 N and in a second step, an additional torque of 6 Nm about the axial direction was added for two more hours. During the whole process, the axial displacement of the top of the spear and its rotation about the axial direction were recorded. The whole experiment was carried out five times emptying and refilling the cavity with new morsellised bone.

A finite element model of the spear with the surrounding layer of impacted bone grafts was created using about 6000 linear tetrahedrons. As the cavity has a rough inner surface, no tangential sliding was allowed. Furthermore the steel cylinder was considered to be of sufficient stiffness to neglect the influence of its deformation on the response of the bone grafts. Hence the interface between the steel cylinder and the bone grafts had no translation and no rotation allowed and the steel cylinder was not modelled. As in the experiment, the force on the

spear was of 1000 N in a first step of 7200 seconds, and then additional torsion of 6 Nm was added for 7200 more seconds.

The material properties were modelled as solid linear viscoelastic and homogeneous. Estimations of the material properties were derived from the first step of the experiments under axial compression. As the steel spear was smoothly polished, we supposed that the main loading mode inside the cavity was compression rather than shear. Thus the experimental data were treated as in a volumetric creep test. The bulk modulus is defined as the ratio of the hydrostatic pressure p_0 to the volumetric strain $\varepsilon^v(t)$:

$$K(t) = \frac{p_0}{\varepsilon^v(t)}$$

Abaqus uses a so-called Prony decomposition of a dimensionless time-dependent bulk modulus:

$$\tilde{K}(t) = \frac{K(t)}{K_0} = \frac{\varepsilon_0^v}{\varepsilon^v(t)} = 1 - \sum_{i=1}^{N} k_i \left[1 - \exp\left(-\frac{t}{\tau_i}\right)\right]$$

where K_0 is the value of $K(t)$ at $t = 0$, ε_0^v is the volumetric strain at $t = 0$, k_i and τ_i are elementary bulk moduli and relaxation times respectively. This expression of the instantaneous bulk modulus can be shown to be equivalent to that obtained for a generalised Kelvin model for viscoelastic solids. This series expansion has a number of terms approximately equal to the 10-logarithm of the duration of the test. Here, a satisfactory approximation ($R^2 = 0.996$) was reached with three terms. The six model parameters, k_i and τ_i, were calculated by the least square method.

Preliminary tests estimated the modulus K_0 from oedometer testing to $K_0 \approx 12$ MPa and triaxial testing evaluated Poisson's ratio ν to $\nu = 0.2$. Based on these values, the final Prony parameters used for the simulation were those summarised in Table 1.

Table 1: The Prony coefficients used for the material model, elementary shear modulus, bulk modulus and relaxation time.

$g_i[-]$	$k_i[-]$	$\tau_i[-]$
0.3942	0.5256	2.102
0.1278	0.1704	79.99
0.0397	0.0529	800

Though the main loading modus of the morsellised bone was assumed to be compression due to the low friction at the spear-bone interface, the friction coefficient had to be estimated to some value. The fluid phase contained in the bone grafts was considered to act like a lubricant. Mechanical handbooks give as lowest values of friction coefficients for greasy polished steel against different materials, approximately 0.1 — apart from Teflon. This value was chosen as a reasonable estimate of the static friction coefficient between the spear and the bone grafts.

3 Results

Of the five repetitions of the experiment, one showed considerably larger displacements than all others, suggesting an error of reset. As nothing could guide us to a reasonable correction, this data series was disregarded for the rest of the study. The remaining four series, represented in Figure 2, show typical creep response in the first step and in the second step separately for the axial displacement and reach about 7 mm in average. The rotation remains around zero in the first step and reaches gradually about 1.3 degrees in the second step in average.

The results of the simulation were recorded as the axial displacement and a transverse displacement converted to rotation angle α by following a corner of the top face of the spear:

$$u_1 = -\frac{b}{2}\sin\alpha \quad \text{or} \quad u_2 = \frac{l}{2}\sin\alpha$$

where u_1 and u_2 are the transverse components of the displacement, l and b are the length and width of the spear section, and α is the rotation angle. As the angles are small we have: $\alpha \approx 2u_2/l$. A comparison of the simulated displacement and rotation with the respective experimental values are plotted in Figure 3. Though the profile of the simulation is qualitatively satisfying and the order of magnitude compared to the experiments is reasonable too, the simulation consequently underestimates both the axial displacement, reaching only 4 mm, and the transverse rotation, reaching about 0.6 degrees.

4 Discussion

This study showed a mismatch between experimentally measured displacement and rotation of the spear and the same simulated quantities, thus suggesting

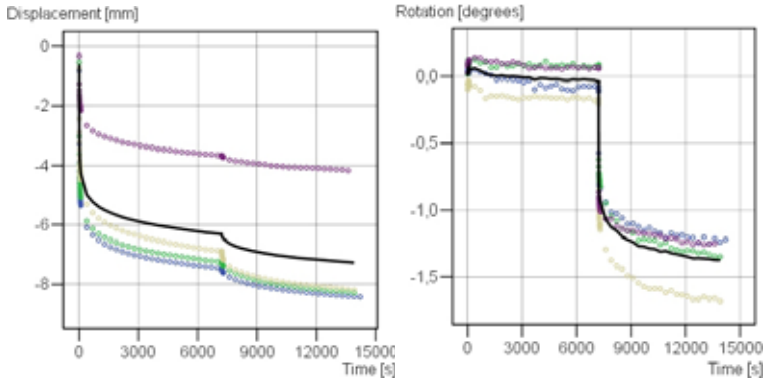

Figure 2: Experimentally measured displacement (left) and rotation (right) of the spear as a function of time for four repetitions of the experiment. The average is plotted as the bold black line.

that a linear viscoelastic solid model is unsuitable to model morsellised bone in these loading conditions.

The nature of morsellised bone is ambivalent. As a pulverulent, it behaves both like a fluid taking the shape of its container and like a solid, as it does not flow out when left on a free surface. Fosse et al. (Paper III, submitted) modelled adequately morsellised bone in a container by a generalised Kelvin model suitable for solid viscoelasticity. Here, the large experimental displacements of the spear suggest an upward flow of morsellised bone because the material at the bottom of the cavity could not be submitted to the strains calculated in pure compression.

If not pre-treated by impaction, the tension strength of morsellised bone is virtually zero as nothing but surface tension of the fluid phase ensures the cohesion of its components. Therefore, the pointy spear would create a stress concentration (estimated to 2.4 MPa in maximum tensile principle stress, using the current model), which would easily overcome the tensile strength of the material. This suggests another approach of the problem using fracture mechanics.

However as very few fracture properties of morsellised bone are known, an alternative approach would be to treat morsellised bone as a viscoelastic fluid, thus allowing it to flow upwards an let the spear penetrate further down. A

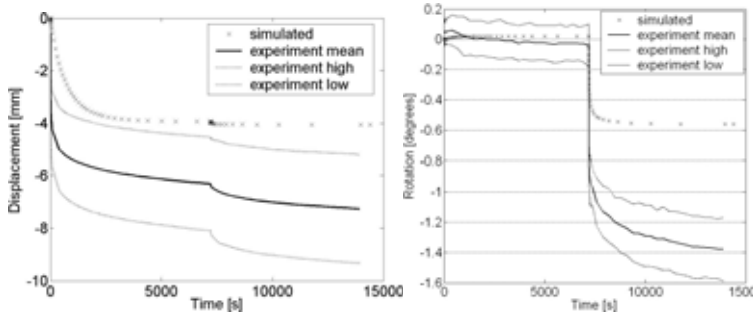

Figure 3: Comparison of simulated displacements and rotations with experimental measurements. The dotted line are one standard deviation from the average.

fluid model would also be suitable in cases where the material is confined in a closed container thus allowing a united modelling of the material.

The frictional properties between the polished steel spear and morsellised bone have to be determined. Simulation with too high friction could be an explanation of the shallower penetration of the spear. But a tentative simulation in the absence of friction produced a different course. A frictionless simulation did indeed not reproduce the acceleration of the axial displacement when the torsion is added. This suggests that this acceleration is caused by a reduction of the frictional forces due to a reduction of the contact surface when the spear is submitted to torsion.

From the discussion above, it is clear that two aspects of the modelling of morsellised bone can be improved: modelling the material as a fluid and calculate the friction coefficient between polished steel and morsellised bone should help providing more satisfying results.

References

Brewster, N.T., Gillespie, W.J., Howie, C.R., Madabhushi, S.P., Usmani, A.S., Fairbairn, D.R., 1999. Mechanical considerations in impaction bone grafting. *J Bone Joint Surg Br* 81, 118-124.

Capello, W.N., 1994. Impaction grafting plus cement for femoral component fixation in revision hip arthroplasty. *Orthopedics* 17, 878-879.

Fosse, L., Muller, S., Rønningen, H., Irgens, F., Benum, P., submitted. Viscoelastic modelling of impacted morsellised bone accurately describes unloading behaviour: an experimental study of stiffness moduli and recoil properties. *J Biomech*

Giesen, E.B., Lamerigts, N.M., Verdonschot, N., Buma, P., Schreurs, B.W., Huiskes, R., 1999. Mechanical characteristics of impacted morsellised bone grafts used in revision of total hip arthroplasty. *J Bone Joint Surg Br* 81, 1052-1057.

Kärrholm, J., Hultmark, P., Carlsson, L., Malchau, H., 1999. Subsidence of a non-polished stem in revisions of the hip using impaction allograft. Evaluation with radiostereometry and dual-energy X-ray absorptiometry. *J Bone Joint Surg Br* 81, 135-142.

Pekkarinen, J., Alho, A., Lepistö, J., Ylikoski, M., Ylinen, P., Paavilainen, T., 2000. Impaction bone grafting in revision hip surgery. A high incidence of complications. *J Bone Joint Surg Br* 82, 103-107.

Ullmark, G., Nilsson, O., 1999. Impacted corticocancellous allografts: recoil and strength. *J Arthroplasty* 14, 1019-1023.

Voor, M.J., White, J.E., Grieshaber, J.E., Malkani, A.L., Ullrich, C.R., 2004. Impacted morselized cancellous bone: mechanical effects of defatting and augmentation with fine hydroxyapatite particles. *J Biomech* 37, 1233-1239.

Zander, T., Rohlmann, A., Klöckner, C., Bergmann, G., 2002a. Comparison of the mechanical behavior of the lumbar spine following mono- and bisegmental stabilization. *Clin Biomech (Bristol, Avon)* 17, 439-445.

Zander, T., Rohlmann, A., Klöckner, C., Bergmann, G., 2002b. Effect of bone graft characteristics on the mechanical behavior of the lumbar spine. *J Biomech* 35, 491-497.

PhD dissertations at the
Department of structural engineering
Norwegian university of science and technology

N-7491 Trondheim, Norway
Telephone: +47 73 59 47 00; Telefax: +47 73 59 47 01

"Reliability Analysis of Structural Systems using Nonlinear Finite Element Methods", C. A. Holm, 1990:23, ISBN 82-7119-178-0.

"Uniform Stratified Flow Interaction with a Submerged Horizontal Cylinder", . Arntsen, 1990:32, ISBN 82-7119-188-8.

"Large Displacement Analysis of Flexible and Rigid Systems Considering Displacement-Dependent Loads and Nonlinear Constraints", K. M. Mathisen, 1990:33, ISBN 82-7119-189-6.

"Solid Mechanics and Material Models including Large Deformations", E. Levold, 1990:56, ISBN 82-7119-214-0, ISSN 0802-3271.

"Inelastic Deformation Capacity of Flexurally-Loaded Aluminium Alloy Structures", T. Welo, 1990:62, ISBN 82-7119-220-5, ISSN 0802-3271.

"Visualization of Results from Mechanical Engineering Analysis", K. Aamnes, 1990:63, ISBN 82-7119-221-3, ISSN 0802-3271.

"Object-Oriented Product Modeling for Structural Design", S. I. Dale, 1991:6, ISBN 82-7119-258-2, ISSN 0802-3271.

"Parallel Techniques for Solving Finite Element Problems on Transputer Networks", T. H. Hansen, 1991:19, ISBN 82-7119-273-6, ISSN 0802-3271.

"Statistical Description and Estimation of Ocean Drift Ice Environments", R. Korsnes, 1991:24, ISBN 82-7119-278-7, ISSN 0802-3271.

"Properties of concrete related to fatigue damage: with emphasis on high strength concrete", G. Petkovic, 1991:35, ISBN 82-7119-290-6, ISSN 0802-3271.

"Turbidity Current Modelling", B. Brørs, 1991:38, ISBN 82-7119-293-0, ISSN 0802-3271.

"Zero-Slump Concrete: Rheology, Degree of Compaction and Strength. Effects of Fillers as Part Cement-Replacement", C. Sørensen, 1992:8, ISBN 82-7119-357-0, ISSN 0802-3271.

"Nonlinear Analysis of Reinforced Concrete Structures Exposed to Transient Loading", K. V. Høiseth, 1992:15, ISBN 82-7119-364-3, ISSN 0802-3271.

"Finite Element Formulations and Solution Algorithms for Buckling and Collapse Analysis of Thin Shells", R. O. Bjrum, 1992:30, ISBN 82-7119-380-5, ISSN 0802-3271.

"Response Statistics of Nonlinear Dynamic Systems", J. M. Johnsen, 1992:42, ISBN 82-7119-393-7, ISSN 0802-3271.

"Digital Models in Engineering. A Study on why and how engineers build and operate digital models for decisison support", J. Høyte, 1992:75, ISBN 82-7119-429-1, ISSN 0802-3271.

"Sparse Solution of Finite Element Equations", A. C. Damhaug, 1992:76, ISBN 82-7119-430-5, ISSN 0802-3271.

"Some Aspects of Floating Ice Related to Sea Surface Operations in the Barents Sea", S. Løset, 1992:95, ISBN 82-7119-452-6, ISSN 0802-3271.

"Modelling of Cyclic Plasticity with Application to Steel and Aluminium Structures", O. S. Hopperstad, 1993:7, ISBN 82-7119-461-5, ISSN 0802-3271.

"The Free Formulation: Linear Theory and Extensions with Applications to Tetrahedral Elements with Rotational Freedoms", G. Skeie, 1993:17, ISBN 82-7119-472-0, ISSN 0802-3271.

"Høyfast betongs motstand mot piggdekkslitasje. Analyse av resultater fra prøving i Veisliter'n", T. Tveter, 1993:62, ISBN 82-7119-522-0, ISSN 0802-3271.

"A Nonlinear Finite Element Based on Free Formulation Theory for Analysis of Sandwich Structures", O. Aamlid, 1993:72, ISBN 82-7119-534-4, ISSN 0802-3271.

"The Effect of Curing Temperature and Silica Fume on Chloride Migration and Pore Structure of High Strength Concrete", C. J. Hauck, 1993:90, ISBN 82-7119-553-0, ISSN 0802-3271.

"Failure of Concrete under Compressive Strain Gradients", G. Markeset, 1993:110, ISBN 82-7119-575-1, ISSN 0802-3271.

"An experimental study of internal tidal amphidromes in Vestfjorden", J. H. Nilsen, 1994:39, ISBN 82-7119-640-5, ISSN 0802-3271.

"Structural analysis of oil wells with emphasis on conductor design", H. Larsen, 1994:46, ISBN 82-7119-648-0, ISSN 0802-3271.

"Adaptive methods for non-linear finite element analysis of shell structures", K. M. Okstad, 1994:66, ISBN 82-7119-670-7, ISSN 0802-3271.

"On constitutive modelling in nonlinear analysis of concrete structures", O. Fyrileiv, 1994:115, ISBN 82-7119-725-8, ISSN 0802-3271.

"Fluctuating wind load and response of a line-like engineering structure with emphasis on motion-induced wind forces", J. Bogunovic Jakobsen, 1995:62, ISBN 82-7119-809-2, ISSN 0802-3271.

"An experimental study of beam-columns subjected to combined torsion, bending and axial actions", A. Aalberg, 1995:66, ISBN 82-7119-813-0, ISSN 0802-3271.

"Scaling and cracking in unsealed freeze/thaw testing of Portland cement and silica fume concretes", S. Jacobsen, 1995:101, ISBN 82-7119-851-3, ISSN 0802-3271.

"Damping of water waves by submerged vegetation. A case study of laminaria hyperborea", A. M. Dubi, 1995:108, ISBN 82-7119-859-9, ISSN 0802-3271.

"The dynamics of a slope current in the Barents Sea", Sheng Li, 1995:109, ISBN 82-7119-860-2, ISSN 0802-3271.

"Modellering av delmaterialenes betydning for betongens konsistens", Ernst Mørtsell, 1996:12, ISBN 82-7119-894-7, ISSN 0802-3271.

"Bending of thin-walled aluminium extrusions", Birgit Søvik Opheim, 1996:60, ISBN 82-7119-947-1, ISSN 0802-3271.

"Material modelling of aluminium for crashworthiness analysis", Torodd Berstad, 1996:89, ISBN 82-7119-980-3, ISSN 0802-3271.

"Estimation of structural parameters from response measurements on submerged floating tunnels", Rolf Magne Larssen, 1996:119, ISBN 82-471-0014-2, ISSN 0802-3271.

"Numerical modelling of plain and reinforced concrete by damage mechanics", Mario A. Polanco-Loria, 1997:20, ISBN 82-471-0049-5, ISSN 0802-3271.

"Nonlinear random vibrations - numerical analysis by path integration methods", Vibeke Moe, 1997:26, ISBN 82-471-0056-8, ISSN 0802-3271.

"Numerical prediction of vortex-induced vibration by the finite element method", Joar Martin Dalheim, 1997:63, ISBN 82-471-0096-7, ISSN 0802-3271.

"Time domain calculations of buffeting response for wind sensitive structures", Ketil Aas-Jakobsen, 1997:148, ISBN 82-471-0189-0, ISSN 0802-3271.

"A numerical study of flow about fixed and flexibly mounted circular cylinders", Trond Stokka Meling, 1998:48, ISBN 82-471-0244-7, ISSN 0802-3271.

"Estimation of chloride penetration into concrete bridges in coastal areas", Per Egil Steen, 1998:89, ISBN 82-471-0290-0, ISSN 0802-3271.

"Stress-resultant material models for reinforced concrete plates and shells", Jan Arve verli, 1998:95, ISBN 82-471-0297-8, ISSN 0802-3271.

"Chloride binding in concrete. Effect of surrounding environment and concrete composition", Claus Kenneth Larsen, 1998:101, ISBN 82-471-0337-0, ISSN 0802-3271.

"Rotational capacity of aluminium alloy beams", Lars A. Moen, 1999:1, ISBN 82-471-0365-6, ISSN 0802-3271.

"Stretch Bending of Aluminium Extrusions", Arild H. Clausen, 1999:29, ISBN 82-471-0396-6, ISSN 0802-3271.

"Aluminium and Steel Beams under Concentrated Loading", Tore Tryland, 1999:30, ISBN 82-471-0397-4, ISSN 0802-3271.

"Engineering Models of Elastoplasticity and Fracture for Aluminium Alloys", Odd-Geir Lademo, 1999:39, ISBN 82-471-0406-7, ISSN 0802-3271.

"Kapasitet og duktilitet av dybelforbindelser i trekonstruksjoner", Jan Siem, 1999:46, ISBN 82-471-0414-8, ISSN 0802-3271.

"Etablering av distribuert ingeniørarbeid; Teknologiske og organisatoriske erfaringer fra en norsk ingeniørbedrift", Lars Line, 1999:52, ISBN 82-471-0420-2, ISSN 0802-3271.

"Estimation of Earthquake-Induced Response", Smon lafsson, 1999:73, ISBN 82-471-0443-1, ISSN 0802-3271.

"Coastal Concrete Bridges: Moisture State, Chloride Permeability and Aging Effects" Ragnhild Holen Relling, 1999:74, ISBN 82-471-0445-8, ISSN 0802-3271.

"Capacity Assessment of Titanium Pipes Subjected to Bending and External Pressure", Arve Bjørset, 1999:100, ISBN 82-471-0473-3, ISSN 0802-3271.

"Validation of Numerical Collapse Behaviour of Thin-Walled Corrugated Panels", Hvar Ilstad, 1999:101, ISBN 82-471-0474-1, ISSN 0802-3271.

"Strength and Ductility of Welded Structures in Aluminium Alloys", Miroslaw Matusiak, 1999:113, ISBN 82-471-0487-3, ISSN 0802-3271.

"Thermal Dilation and Autogenous Deformation as Driving Forces to Self-Induced Stresses in High Performance Concrete", yvind Bjøntegaard, 1999:121, ISBN 82-7984-002-8, ISSN 0802-3271.

"Some Aspects of Ski Base Sliding Friction and Ski Base Structure", Dag Anders Moldestad, 1999:137, ISBN 82-7984-019-2, ISSN 0802-3271.

"Electrode reactions and corrosion resistance for steel in mortar and concrete", Roy Antonsen, 2000:10, ISBN 82-7984-030-3, ISSN 0802-3271.

"Hydro-Physical Conditions in Kelp Forests and the Effect on Wave Damping and Dune Erosion. A case study on Laminaria Hyperborea", Stig Magnar Løvs, 2000:28, ISBN 82-7984-050-8, ISSN 0802-3271.

"Random Vibration and the Path Integral Method", Christian Skaug, 2000:39, ISBN 82-7984-061-3, ISSN 0802-3271.

"Buckling and geometrical nonlinear beam-type analyses of timber structures", Trond Even Eggen, 2000:56, ISBN 82-7984-081-8, ISSN 0802-3271.

"Structural Crashworthiness of Aluminium Foam-Based Components", Arve Grønsund Hanssen, 2000:76, ISBN 82-7984-102-4, ISSN 0809-103X.

"Measurements and simulations of the consolidation in first-year sea ice ridges, and some aspects of mechanical behaviour", Knut V. Høyland, 2000:94, ISBN 82-7984-121-0, ISSN 0809-103X.

"Kinematics in Regular and Irregular Waves based on a Lagrangian Formulation", Svein Helge Gjøsund, 2000-86, ISBN 82-7984-112-1, ISSN 0809-103X.

"Self-Induced Cracking Problems in Hardening Concrete Structures", Daniela Bosnjak, 2000-121, ISBN 82-7984-151-2, ISSN 0809-103X.

"Ballistic Penetration and Perforation of Steel Plates", Tore Børvik, 2000:124, ISBN 82-7984-154-7, ISSN 0809-103X.

"Freeze-Thaw resistance of Concrete. Effect of: Curing Conditions, Moisture Exchange and Materials", Terje Finnerup Rønning, 2001:14, ISBN 82-7984-165-2, ISSN 0809-103X.

Structural behaviour of post tensioned concrete structures. Flat slab. Slabs on ground", Steinar Trygstad, 2001:52, ISBN 82-471-5314-9, ISSN 0809-103X.

"Slipforming of Vertical Concrete Structures. Friction between concrete and slipform panel", Kjell Tore Foss, 2001:61, ISBN 82-471-5325-4, ISSN 0809-103X.

"Some numerical methods for the simulation of laminar and turbulent incompressible flows", Jens Holmen, 2002:6, ISBN 82-471-5396-3, ISSN 0809-103X.

"Improved Fatigue Performance of Threaded Drillstring Connections by Cold Rolling", Steinar Kristoffersen, 2002:11, ISBN: 82-421-5402-1, ISSN 0809-103X.

"Deformations in Concrete Cantilever Bridges: Observations and Theoretical Modelling", Peter F. Takcs, 2002:23, ISBN 82-471-5415-3, ISSN 0809-103X.

"Stiffened aluminium plates subjected to impact loading", Hilde Giver Hildrum, 2002:69, ISBN 82-471-5467-6, ISSN 0809-103X.

"Full- and model scale study of wind effects on a medium-rise building in a built up area", Jnas Thr Snbjørnsson, 2002:95, ISBN82-471-5495-1, ISSN 0809-103X.

"Evaluation of Concepts for Loading of Hydrocarbons in Ice-infested water", Arnor Jensen, 2002:114, ISBN 82-417-5506-0, ISSN 0809-103X.

"Numerical and Physical Modelling of Oil Spreading in Broken Ice", Janne K. kland Gjøsteen, 2002:130, ISBN 82-471-5523-0, ISSN 0809-103X.

"Diagnosis and protection of corroding steel in concrete", Franz Pruckner, 20002:140, ISBN 82-471-5555-4, ISSN 0809-103X.

"Tensile and Compressive Creep of Young Concrete: Testing and Modelling", Dawood Atrushi, 2003:17, ISBN 82-471-5565-6, ISSN 0809-103X.

"Rheology of Particle Suspensions. Fresh Concrete, Mortar and Cement Paste with Various Types of Lignosulfonates", Jon Elvar Wallevik, 2003:18, ISBN 82-471-5566-4, ISSN 0809-103X.

"Oblique Loading of Aluminium Crash Components", Aase Reyes, 2003:15, ISBN 82-471-5562-1, ISSN 0809-103X.

"Utilization of Ethiopian Natural Pozzolans", Surafel Ketema Desta, 2003:26, ISSN 82-471-5574-5, ISSN:0809-103X.

"Behaviour and strength prediction of reinforced concrete structures with discontinuity regions", Helge Br, 2004:11, ISBN 82-471-6222-9, ISSN 1503-8181.

"High-strength steel plates subjected to projectile impact. An experimental and numerical study", Sumita Dey, 2004:38, ISBN 82-471-6281-4 (elektr. Utg.), ISBN 82-471-6282-2 (trykt utg.), ISSN 1503-8181.

"Alkali-reactive and inert fillers in concrete. Rheology of fresh mixtures and expansive reactions." Brd M. Pedersen, 2004:92, ISBN 82-471-6401-9 (trykt utg.), ISBN 82-471-6400-0 (elektr. utg.), ISSN 1503-8181.

"On the Shear Capacity of Steel Girders with Large Web Openings". Nils Christian Hagen, 2005:9 ISBN 82-471-6878-2 (trykt utg.), ISBN 82-471-6877-4 (elektr. utg.), ISSN 1503-8181.

"Behaviour of aluminium extrusions subjected to axial loading". sten Jensen, 2005:7, ISBN 82-471-6872-3 (elektr. utg.) , ISBN 82-471-6873-1 (trykt utg.), ISSN 1503-8181.

"Thermal Aspects of corrosion of Steel in Concrete". Jan-Magnus stvik, 2005:5, ISBN 82-471-6869-3 (trykt utg.) ISBN 82-471-6868 (elektr.utg), ISSN 1503-8181.